

# Geometry of the quasi-hyperbolic Szekeres models

Andrzej Krasiński

*N. Copernicus Astronomical Centre,  
Polish Academy of Sciences,  
Bartycka 18, 00 716 Warszawa, Poland\**

Krzysztof Bolejko

*Sydney Institute for Astronomy, School of Physics A28,  
The University of Sydney, NSW 2006, Australia†*

(Dated:)

Geometric properties of the quasi-hyperbolic Szekeres models are discussed and related to the quasi-spherical Szekeres models. Typical examples of shapes of various classes of 2-dimensional coordinate surfaces are shown in graphs; for the hyperbolically symmetric subcase and for the general quasi-hyperbolic case. An analysis of the mass function  $M(z)$  is carried out in parallel to an analogous analysis for the quasi-spherical models. This leads to the conclusion that  $M(z)$  determines the density of rest mass averaged over the whole space of constant time.

PACS numbers:

Keywords:

## I. MOTIVATION

Continuing the research started in Refs. [1] and [2], the geometry of the quasi-hyperbolic Szekeres models is investigated. Unlike the quasi-spherical Szekeres models that have been extensively investigated [3] – [20] and are rather well-understood by now, the quasi-plane and quasi-hyperbolic models are still poorly explored. This situation has somewhat improved recently: in Ref. [1] a preliminary investigation of the geometry of both these classes was carried out, and in Ref. [2] it was shown that the physical interpretation of the plane symmetric models becomes clearer when a torus topology is assumed for the orbits of their symmetry.

The present paper is an attempt to understand the geometry of the quasi-hyperbolic model. In Sec. II the full set of the  $\beta_{,z} \neq 0$  Szekeres solutions is presented. In Sec. III limitations for the arbitrary functions in the quasi-hyperbolic models are discussed that result from the spacetime signature and from the evolution equation. It is also shown that a set where the mass function is zero is allowed to exist. In Sec. IV it is recalled after Ref. [2] that the quasi-hyperbolic Szekeres manifold is all contained within an apparent horizon, i.e. is globally trapped. In Sec. VI the geometry of various 2-dimensional surfaces in the hyperbolically symmetric subcase is investigated and illustrated with graphs. In Sec. VII it is shown what deformations to the surfaces of constant  $t$  and  $\varphi$  ensue in the general quasi-hyperbolic case. In Secs. VIII – XI various properties of the mass function in the quasi-spherical models are discussed, in order to prepare the ground for an analogous discussion

of the quasi-hyperbolic case. This latter task is carried out in Secs. XII and XIII. The purpose of this was to identify the volume in a space of constant  $t$ , which could be related to the mass  $M(z)$ . This goal was not achieved as intended, but it was shown that  $M(z)$  determines the density of rest mass averaged over the space of constant time. Section XIV is a summary of the results.

The aim of this paper is to advance the insight into the geometry of this class of spacetimes. This is supposed to be the next step after the exploratory investigation done in Ref. [1].

## II. INTRODUCING THE SZEKERES SOLUTIONS

This section is mostly copied from Ref. [2], mainly in order to define the notation.

The metric of the Szekeres solutions is

$$ds^2 = dt^2 - e^{2\alpha} dz^2 - e^{2\beta} (dx^2 + dy^2), \quad (2.1)$$

where  $\alpha$  and  $\beta$  are functions of  $(t, x, y, z)$  to be determined from the Einstein equations with a dust source. The coordinates of (2.1) are comoving, so the velocity field of the dust is  $u^\mu = \delta^\mu_0$ , and  $\dot{u}^\mu = 0$ .

There are in fact two families of Szekeres solutions, depending on whether  $\beta_{,z} = 0$  or  $\beta_{,z} \neq 0$ . The first family is a simultaneous generalisation of the Friedmann and Kantowski – Sachs [21] models. Since so far it has found no useful application in astrophysical cosmology, we shall not discuss it here (see Ref. [17]), and we shall deal only with the second family.

After the Einstein equations are solved, the metric functions in (2.1) become

$$\begin{aligned} e^\beta &= \Phi(t, z) e^{\nu(z, x, y)}, \\ e^\alpha &= h(z) \Phi(t, z) \beta_{,z} \equiv h(z) (\Phi_{,z} + \Phi \nu_{,z}), \end{aligned} \quad (2.2)$$

\*Electronic address: akr@camk.edu.pl

†Electronic address: bolejko@physics.usyd.edu.au

$$e^{-\nu} = A(z)(x^2 + y^2) + 2B_1(z)x + 2B_2(z)y + C(z),$$

where  $\Phi(t, z)$  is a solution of the equation

$$\Phi_{,t}^2 = -k(z) + \frac{2\widetilde{M}(z)}{\Phi} + \frac{1}{3}\Lambda\Phi^2; \quad (2.3)$$

while  $h(z)$ ,  $k(z)$ ,  $\widetilde{M}(z)$ ,  $A(z)$ ,  $B_1(z)$ ,  $B_2(z)$  and  $C(z)$  are arbitrary functions obeying

$$g(z) \stackrel{\text{def}}{=} 4(AC - B_1^2 - B_2^2) = 1/h^2(z) + k(z). \quad (2.4)$$

The mass-density  $\rho$  is

$$\kappa\rho c^2 = \frac{(2\widetilde{M}e^{3\nu})_{,z}}{e^{2\beta}(e^\beta)_{,z}}; \quad \kappa = 8\pi G/c^4. \quad (2.5)$$

This family of solutions has in general no symmetry, and acquires a 3-dimensional symmetry group with 2-dimensional orbits when  $A$ ,  $B_1$ ,  $B_2$  and  $C$  are constant (then  $\nu_{,z} = 0$ ). The sign of  $g(z)$  determines the geometry of the surfaces of constant  $t$  and  $z$  and the symmetry of the  $\nu_{,z} = 0$  subcase. The geometry is spherical, plane or hyperbolic when  $g > 0$ ,  $g = 0$  or  $g < 0$ , respectively. With  $A$ ,  $B_1$ ,  $B_2$  and  $C$  being functions of  $z$ , the surfaces  $z = \text{const}$  within a single space  $t = \text{const}$  may have different geometries, i.e. they can be spheres in one part of the space and surfaces of constant negative curvature elsewhere, the curvature being zero at the boundary – see a simple example of this situation in Ref. [1].<sup>1</sup> The sign of  $k(z)$  determines the type of evolution when  $\Lambda = 0$ ; with  $k > 0$  the model expands away from an initial singularity and then recollapses to a final singularity, with  $k < 0$  the model is ever-expanding or ever-collapsing, depending on the initial conditions;  $k = 0$  is the intermediate case with expansion velocity tending to zero asymptotically.

The Szekeres models are subdivided according to the sign of  $g(z)$  into quasi-spherical (with  $g > 0$ ), quasi-plane ( $g = 0$ ) and quasi-hyperbolic ( $g < 0$ ). The geometry of the latter two classes has, until recently, not been investigated and is not really understood; work on their interpretation was only begun by Hellaby and Krasiński [1], and somewhat advanced for the quasi-plane models by the present author [2]. The sign of  $g(z)$  imposes limitations on the sign of  $k(z)$ . For the signature to be the physical (+ – – –), the function  $h^2$  must be non-negative (possibly zero at isolated points, but not in open subsets), which, via (2.4), means that  $g(z) - k(z) \geq 0$  everywhere. Thus, with  $g > 0$  all three possibilities for  $k$  are allowed; with  $g = 0$  only the two  $k \leq 0$  evolutions are admissible ( $k = 0$  only at isolated values of  $z$ ), and with  $g < 0$ , only the  $k < 0$  evolution is allowed.

The quasi-spherical models may be imagined as such generalisations of the Lemaître – Tolman (L–T) model

in which the spheres of constant mass are non-concentric. The functions  $A(z)$ ,  $B_1(z)$  and  $B_2(z)$  determine how the center of a sphere changes its position in a space  $t = \text{const}$  when the radius of the sphere is increased [16].

Often, it is practical to reparametrise the arbitrary functions in the Szekeres metric as follows [22]. Even if  $A = 0$  initially, a transformation of the  $(x, y)$ -coordinates can restore  $A \neq 0$ , so we may assume  $A \neq 0$  with no loss of generality [17]. Then let  $g \neq 0$ . Writing

$$(A, B_1, B_2) = \frac{\sqrt{|g|}}{2S}(1, -P, -Q), \quad \varepsilon \stackrel{\text{def}}{=} g/|g|, \quad (2.6)$$

$$k = -|g| \times 2E, \quad \widetilde{M} = |g|^{3/2}M, \quad \Phi = \sqrt{|g|R},$$

we can represent the metric (2.1) as

$$\frac{e^{-\nu}}{\sqrt{|g|}} \stackrel{\text{def}}{=} \mathcal{E} \stackrel{\text{def}}{=} \frac{S}{2} \left[ \left( \frac{x-P}{S} \right)^2 + \left( \frac{y-Q}{S} \right)^2 + \varepsilon \right], \quad (2.7)$$

$$ds^2 = dt^2 - \frac{(R_{,z} - R\mathcal{E}_{,z}/\mathcal{E})^2}{\varepsilon + 2E(z)} dz^2 - \frac{R^2}{\mathcal{E}^2} (dx^2 + dy^2). \quad (2.8)$$

When  $g = 0$ , the transition from (2.1) to (2.7) – (2.8) is  $A = 1/(2S)$ ,  $B_1 = -P/(2S)$ ,  $B_2 = -Q/(2S)$ ,  $k = -2E$ ,  $\widetilde{M} = M$  and  $\Phi = R$ . Then (2.7) – (2.8) applies with  $\varepsilon = 0$ , and the resulting model is quasi-plane.

Equation (2.3), in the variables of (2.8) becomes

$$R_{,t}^2 = 2E(z) + \frac{2M(z)}{R} + \frac{1}{3}\Lambda R^2; \quad (2.9)$$

From now on, we will use this representation. The formula for density in these variables is

$$\kappa\rho c^2 = \frac{2(M_{,z} - 3M\mathcal{E}_{,z}/\mathcal{E})}{R^2(R_{,z} - R\mathcal{E}_{,z}/\mathcal{E})}. \quad (2.10)$$

For  $\rho > 0$ ,  $(M_{,z} - 3M\mathcal{E}_{,z}/\mathcal{E})$  and  $(R_{,z} - R\mathcal{E}_{,z}/\mathcal{E})$  must have the same sign. Note that the sign of both these expressions may be flipped by the transformation  $z \rightarrow -z$ , so we may assume that

$$R_{,z} - R\mathcal{E}_{,z}/\mathcal{E} > 0 \quad (2.11)$$

at least somewhere. In this preliminary investigation we assume that we are in that part of the manifold, where (2.11) holds.

In (2.7) – (2.8) the arbitrary functions are independent.<sup>2</sup> However, (2.7) – (2.8) creates the illusion that the values  $\varepsilon = +1, 0, -1$  characterise the whole spacetime, while in truth all three cases can occur in the same spacetime.

<sup>1</sup> In most of the literature, these models have been considered separately, but this was only for purposes of systematic research.

<sup>2</sup> Equation (2.4) defines  $C = \sqrt{|g|}[(P^2 + Q^2)/S + \varepsilon S]/2$ .

Within each single  $\{t = \text{const}, z = \text{const}\}$  surface, in the case  $\varepsilon = +1$ , the  $(x, y)$  coordinates of (2.1) can be transformed to the spherical  $(\vartheta, \varphi)$  coordinates by

$$(x - P, y - Q)/S = \cot(\vartheta/2)(\cos \varphi, \sin \varphi). \quad (2.12)$$

This transformation is called a *stereographic projection*. For its geometric interpretation and for the corresponding formulae in the  $\varepsilon \leq 0$  cases see Refs. [1] and [17].

The shear tensor for the Szekeres models is [17]

$$\sigma^\alpha_\beta = \frac{1}{3}\Sigma \text{diag}(0, 2, -1, -1), \quad \text{where} \\ \Sigma = \frac{R_{,tz} - R_{,t} R_{,z}/R}{R_{,z} - R\mathcal{E}_{,z}/\mathcal{E}}. \quad (2.13)$$

Since rotation and acceleration are zero, the limit  $\sigma^\alpha_\beta \rightarrow 0$  must be the Friedmann model [17, 23]. In this limit we have

$$R(t, z) = r(z)S(t), \quad (2.14)$$

and then (2.9) implies that

$$E/r^2, M/r^3 \text{ and } t_B(z) \text{ are all constant.} \quad (2.15)$$

However, with  $P(z)$ ,  $Q(z)$  and  $S(z)$  still being arbitrary, the resulting coordinate representation of the Friedmann model is very untypical. The more usual coordinates result when

$$P_{,z} = Q_{,z} = S_{,z} = 0, \quad (2.16)$$

and  $r(z)$  is chosen as the  $z'$ -coordinate. (We stress that this is achieved simply by coordinate transformation, but writing it out explicitly is an impossible task.) However, (2.14) and (2.16) substituted in (2.8) give the standard representation of the Friedmann model only when  $\varepsilon = +1$ . With  $\varepsilon = 0$  and  $\varepsilon = -1$ , further transformations are needed to obtain the familiar form [1, 24, 25].

The above is a minimal body of information about the Szekeres models needed to follow the remaining part of this paper. More extended presentations of physical and geometrical properties of these models can be found in Refs. [1, 2, 16–19].

### III. SPECIFIC PROPERTIES OF THE QUASI-HYPERBOLIC MODEL

From now on we consider only the case  $\Lambda = 0$ ,  $\varepsilon = -1$  and only expanding models. The corresponding conclusions for collapsing models follow immediately.

It was stated in Ref. [1] that the surfaces  $\mathcal{H}_2$  of constant  $t$  and  $z$  in (2.8) in the quasi-hyperbolic case  $\varepsilon = -1$  consist of two disjoint sheets. This was a conclusion from the fact that with  $\varepsilon = -1$  the equation  $\mathcal{E} = 0$  has a solution for  $(x, y)$  at every value of  $z$ , and every curve that goes into the set  $\mathcal{E} = 0$  has infinite length. However, it will be shown in Sec. VI that the two sheets are in fact

two coverings of the same surface, also in the general non-symmetric case. Their spurious isolation is a property of the stereographic coordinates used in (2.8).

Note that with  $\varepsilon = -1$  (2.8) shows that for the signature to be the physical  $(+ - - -)$ ,

$$E(z) \geq 1/2, \quad (3.1)$$

is necessary, with  $E = 1/2$  being possible at isolated values of  $z$ , but not on open subsets. We shall also assume

$$M(z) \geq 0 \quad (3.2)$$

for all  $z$ , since with  $M < 0$  (2.9) would imply  $R_{,tt} > 0$ , i.e. decelerated collapse or accelerated expansion, which means gravitational repulsion.

In consequence of (3.1), only one class of solutions of (2.9) is possible in the quasi-hyperbolic case:

$$R = \frac{M}{2E} (\cosh \eta - 1), \\ t - t_B = \frac{M}{(2E)^{3/2}} (\sinh \eta - \eta). \quad (3.3)$$

The second of the above determines  $\eta$  as a function of  $t$ , with  $z$  being an arbitrary parameter, and then the first equation determines  $R(t, z)$ .

Equations (3.1), (3.2) and (2.9) with  $\Lambda = 0$  imply that  $R_{,t}^2 > 0$  at all  $z$ , i.e. there can be no location in the manifold at which  $R_{,t} = 0$ . In particular, there exists no location at which  $R = 0$  permanently. The function  $R$  attains the value 0 only at  $t = t_B$ , i.e. at the Big Bang. We have, at all points where  $M > 0$ ,

$$\lim_{t \rightarrow t_B} R(t, z) = 0, \quad \lim_{t \rightarrow t_B} R_{,t}(t, z) = \infty, \quad (3.4)$$

but  $R > 0$  at all values of  $z$  where  $t > t_B$ . Thus, in the quasi-hyperbolic model there exists no analogue of the origin of the quasi-spherical model or of the center of symmetry of the spherically symmetric model. (This fact was demonstrated in Ref. [1] by a different method.)

However, a location  $z = z_{m0}$  at which  $M(z_{m0}) = 0$  is not prohibited, even though the parameter  $\eta$  in (3.3) becomes undetermined when  $M = 0 \neq E$ . Writing the solution of (3.3) as

$$t - t_B = \frac{M}{(2E)^{3/2}} \left[ \sqrt{4E^2 R^2 / M^2 + 4ER/M} \right. \\ \left. - \ln \left( 2ER/M + 1 + \sqrt{4E^2 R^2 / M^2 + 4ER/M} \right) \right] \quad (3.5)$$

(where the log-term is the function inverse to cosh) we

see that the limit of this as  $M \rightarrow 0$  is<sup>3</sup>

$$\lim_{z \rightarrow z_{m_0}} (t - t_B) = \frac{R}{\sqrt{2E}} \Big|_{z=z_{m_0}}, \quad (3.6)$$

and the same result follows from (2.9) with  $M = 0 = \Lambda$ .

Note that (3.6) implies  $R_{,t}(t, z_{m_0}) = \sqrt{2E(z_{m_0})}$  – an expansion rate independent of time. This agrees with Newtonian intuition – expansion under the influence of zero mass should proceed with zero acceleration. At all other locations, where  $M(z) > 0$ , the expansion rate is greater than  $\sqrt{2E(z)}$ , and tends to  $\sqrt{2E(z)}$  only at  $R(t, z) \rightarrow \infty$ . However,  $E(z)$  at  $z \neq z_{m_0}$  may be smaller than  $E(z_{m_0})$ , so the expansion rate in the neighbourhood of the  $M = 0$  set may in fact be *smaller* than  $\sqrt{2E(z_{m_0})}$ .

Conversely, at a location where  $R_{,t} = \text{constant}$  (with  $\Lambda = 0$ ), (2.9) implies that  $M = 0$  (because  $R_{,t} \neq 0$  in consequence of  $E \geq 1/2$ ,  $M \geq 0$  and  $R \geq 0$ ).

The set where  $M = 0$  may or may not exist in a given quasi-hyperbolic Szekeres spacetime. It should be noted that, if it exists, it is a 3-dimensional hypersurface in spacetime; unlike the origin in the quasi-spherical models. The latter is a 2-dimensional surface in spacetime and a single point in each space of constant  $t$  because in the quasi-spherical case  $M = 0$  implies  $R = 0$  via the regularity conditions.

#### IV. NO APPARENT HORIZONS

In Ref. [2] it was shown that a collapsing quasi-hyperbolic Szekeres manifold is all contained within the future apparent horizon, i.e. that it represents the interior of a black hole. This is consistent with the fact that the corresponding vacuum solution (the hyperbolically symmetric counterpart of the Schwarzschild solution) has no event horizons and is globally nonstatic [1].

Here, we consider expanding models, and an addendum is needed to the result reported above. Consider a surface of constant  $t$  and  $z$  in (2.8), and a family of null geodesics intersecting it orthogonally. As shown in Refs. [2] and [16], the expansion scalar for this family is

$$k^\mu{}_{;\mu} = 2 \left| \frac{R_{,z}}{R} - \frac{\mathcal{E}_{,z}}{\mathcal{E}} \right| \left( \frac{R_{,t}}{\sqrt{2E-1}} + e \right), \quad (4.1)$$

where  $e = +1$  for “outgoing” and  $e = -1$  for “ingoing” geodesics;<sup>4</sup> eq. (4.1) was adapted to  $\varepsilon = -1$ .

For an expanding model  $R_{,t} > 0$ , and only past-trapped surfaces can possibly exist, for which  $k^\mu{}_{;\mu} > 0$ . Apart from shell crossings the first factor in (4.1) is positive everywhere. Hence, (4.1) implies

$$\frac{R_{,t}}{\sqrt{2E-1}} + e > 0. \quad (4.2)$$

For  $e = +1$ , and with  $R_{,t} > 0$  that we now consider, this is fulfilled everywhere. For  $e = -1$  we get

$$R_{,t}^2 > 2E - 1 \geq 0 \quad (4.3)$$

(the last inequality from (3.1)). With  $\Lambda = 0$ , (4.3) is also guaranteed to hold everywhere, by (2.9), since  $M \geq 0$  and  $R \geq 0$ . This means that every surface of constant  $t$  and  $z$  in an expanding model is past-trapped at all of its points. But then, every point of the Szekeres manifold lies within one such surface. This, in turn, means that every point of the Szekeres manifold is within a past-trapped region. Therefore, the whole quasi-hyperbolic expanding Szekeres manifold is within a past apparent horizon.

The fact of being globally trapped is a serious limitation on the possible astrophysical applications of the quasi-hyperbolic model.

#### V. INTERPRETATION OF THE COORDINATES OF (2.8)

In order to understand the geometry of (2.8), we begin with the hyperbolically symmetric subcase,  $P_{,z} = Q_{,z} = S_{,z} = 0$ . It is most conveniently represented as

$$ds^2 = dt^2 - \frac{R_{,z}^2 dz^2}{2E-1} - R^2 (d\vartheta^2 + \sinh^2 \vartheta d\varphi^2). \quad (5.1)$$

The two supposedly disjoint sheets of a constant- $(t, z)$  surface, in the coordinates of (2.8), are

$$\begin{aligned} \text{Sheet 1: } & \left( \frac{x-P}{S} \right)^2 + \left( \frac{y-Q}{S} \right)^2 > 1, \\ \text{Sheet 2: } & \left( \frac{x-P}{S} \right)^2 + \left( \frac{y-Q}{S} \right)^2 < 1. \end{aligned} \quad (5.2)$$

The transformation from Sheet 1 to (5.1) is

$$(x, y) = (P, Q) + S \coth(\vartheta/2) (\cos \varphi, \sin \varphi), \quad (5.3)$$

while the transformation from Sheet 2 is

$$(x, y) = (P, Q) + S \tanh(\vartheta/2) (\cos \varphi, \sin \varphi). \quad (5.4)$$

This shows that the two sheets are in truth two coordinate coverings of the same surface. The direct coordinate transformation between the two sheets is the inversion

$$(x - P, y - Q) = \frac{S^2 (x' - P, y' - Q)}{(x' - P)^2 + (y' - Q)^2}. \quad (5.5)$$

<sup>3</sup> The result (3.6) shows that the argument used in deriving the regularity conditions at the center for the Lemaitre – Tolman model in Ref. [26], and repeated in Sec. 18.4 of Ref. [17], was incorrect. The value of the parameter  $\eta$  need not be determined at the center. However, the resulting regularity conditions are correct because they can be derived in a different way. Once we know that  $R = 0$ ,  $M = 0$  and  $R \propto M^{1/3}$  at the center, the behaviour of  $E$  at the center follows from eq. (2.9).

<sup>4</sup> Since the surfaces of constant  $t$  and  $z$  are infinite, this labelling is purely conventional in this case, but the two families are distinct.

The circle separating the two sheets,  $(x - P)^2 + (y - Q)^2 = S^2$ , on which  $\mathcal{E} = 0$ , corresponds to  $\vartheta \rightarrow \pm\infty$  in the coordinates of (5.1). The center of this circle,  $(x, y) = (P, Q)$ , which is in Sheet 2, is mapped by (5.4) to  $\vartheta = 0$ . The infinity,  $(x - P)^2 + (y - Q)^2 \rightarrow \infty$ , which is in Sheet 1, is mapped by (5.3) also to  $\vartheta = 0$ . These relations are illustrated in Fig. 1.

There is no reason to allow negative values of  $\vartheta$  in (5.1) because, as both (5.3) and (5.4) show, the point of coordinates  $(-\vartheta, \varphi)$  coincides with the point of coordinates  $(\vartheta, \varphi + \pi)$ , so the ranges  $\vartheta \in [0, +\infty)$  and  $\varphi \in [0, 2\pi)$  cover the whole  $(\vartheta, \varphi)$  surface.

Curves that go through  $\vartheta = 0$  are seen from (5.1) to have finite length. At  $\vartheta = 0$  we have  $\det(g_{\alpha\beta}) = 0$ , but the curvature scalars given in Appendix A do not depend on  $\vartheta$ , so  $\vartheta = 0$  is only a coordinate singularity.

The geometry of the  $(x, y)$  surfaces in (2.8) is the same in the hyperbolically symmetric case and in the full non-symmetric case with  $\mathcal{E}_{,z} \neq 0$ . In the  $(x, y)$  coordinates of (2.8),  $\vartheta = 0$  corresponds to  $\mathcal{E} = -1$  in Sheet 2, which is clearly not a singularity, and to  $\mathcal{E} \rightarrow \infty$  in Sheet 1. This seems to be a singularity in (2.8), but the curvature scalars are not singular there, as shown in Appendix B. Also the set  $\mathcal{E} = 0$  seems to be singular in (2.8), but the same formulae in Appendix B show that it is nonsingular. Hence, also in the general case there is no reason to treat these two sheets as disjoint – they are two coordinate coverings of the same surface.

## VI. GEOMETRY OF SUBSPACES IN THE HYPERBOLICALLY SYMMETRIC LIMIT

### A. Hypersurfaces of constant $z$

A hypersurface  $z = z_1 = \text{constant}$  has the curvature tensor:

$$\begin{aligned} {}^3R_{0202} &= {}^3R_{0303}/\sinh^2\vartheta = RR_{,tt}, \\ {}^3R_{2323} &= R^2 \sinh^2\vartheta (1 - R_{,t}^2), \end{aligned} \quad (6.1)$$

where  $(x^0, x^2, x^3) = (t, \vartheta, \varphi)$ . Consequently, it is flat when  $R_{,t} = \pm 1$  and curved in every other case (also when  $R_{,t} = \text{constant} \neq \pm 1$ ). However, (2.9) implies that with  $R_{,t} = \pm 1$  we have  $M = 0$  and  $E = 1/2$  (recall: we consider only the case  $\Lambda = 0$ ). Such a subset in spacetime (if it exists) is a special case of a neck – see the explanation to Fig. 10 later in this section.

The metric of a general hypersurface of constant  $z$  is

$$ds_{z_1}^2 = dt^2 - R^2(t, z_1) (d\vartheta^2 + \sinh^2\vartheta d\varphi^2). \quad (6.2)$$

To gain insight into its geometry, we first consider its subspace given by  $\varphi = \varphi_0 = \text{constant}$ . The  $z_1$  is a constant parameter within  $R$  and will be omitted in the formulae below. The corresponding 2-dimensional metric is

$$ds_{z_1, \varphi_0}^2 = dt^2 - R^2(t) d\vartheta^2 \equiv \left(\frac{dt}{dR}\right)^2 dR^2 - R^2 d\vartheta^2. \quad (6.3)$$

This can be embedded in a flat 3-dimensional Minkowskian space with the metric

$$ds_M^2 = dT^2 - dX^2 - dY^2 \quad (6.4)$$

by

$$\begin{aligned} T &= \int \sqrt{1 + \left(\frac{dt}{dR}\right)^2} dR, \\ X &= R \cos\vartheta, \quad Y = R \sin\vartheta. \end{aligned} \quad (6.5)$$

The embedding (6.5) projects a point of coordinates  $(R, \vartheta)$  and points of coordinates  $(R, \vartheta + 2\pi n)$ , where  $n$  is any integer, onto the same point of the Minkowskian space (6.4). However, these points do not coincide in the spacetime (5.1) – the identification of  $(R, \vartheta)$  with  $(R, \vartheta + 2\pi)$  is not allowed because the transformation  $\vartheta \rightarrow \vartheta + 2\pi$  is not an isometry in (5.1). Thus, the surface with the metric (6.3) is covered by the mapping (6.5) an infinite number of times. This shows that a hyperbolically symmetric geometry is a rather exotic and complicated entity. We shall see this feature further on, while considering other surfaces.

Using (2.9) with  $\Lambda = 0$  we can write

$$\left(\frac{dt}{dR}\right)^2 = \frac{R}{2ER + 2M}, \quad (6.6)$$

and then the integral in (6.5) can be calculated explicitly:

$$T = \frac{FG}{2E} - \frac{M}{E\sqrt{2E(2E+1)}} \ln\left(\sqrt{2EF} + \sqrt{2E+1}G\right) + D, \quad (6.7)$$

where  $D$  is a constant and

$$F \stackrel{\text{def}}{=} \sqrt{(2E+1)R + 2M}, \quad G \stackrel{\text{def}}{=} \sqrt{2ER + 2M}. \quad (6.8)$$

The constant  $D$  can be chosen so that  $T = 0$  at  $R = 0$ . Figure 2 shows the graph of the surface given by the parametric equations (6.5) as embedded in the 3-dimensional space with the metric (6.4). It is not exactly a cone, the curves  $T(R)$  do have nonzero curvature

$$\frac{d^2T}{dR^2} = \frac{M}{FG^3}, \quad (6.9)$$

but it is so small everywhere that it would not show up in a graph. Note that the vertex angle of this conical surface is everywhere larger than  $\pi/4$ , since  $dT/dR > 1$  from (6.5).

Suppose that we made  $T$  unique by choosing  $D$  as indicated under (6.8). The vertex of the conical surface in Fig. 2 corresponds to the Big Bang. If we want the image in this figure to correspond to the history of the Universe from the Big Bang up to now, then the upper edge of the funnel should be at  $T(R_p)$ , where  $R_p$  corresponds to the present moment. But this  $R_p$  depends on the value of  $z = z_1$ . Consequently, the height of the funnel will be different at different values of  $z$ .

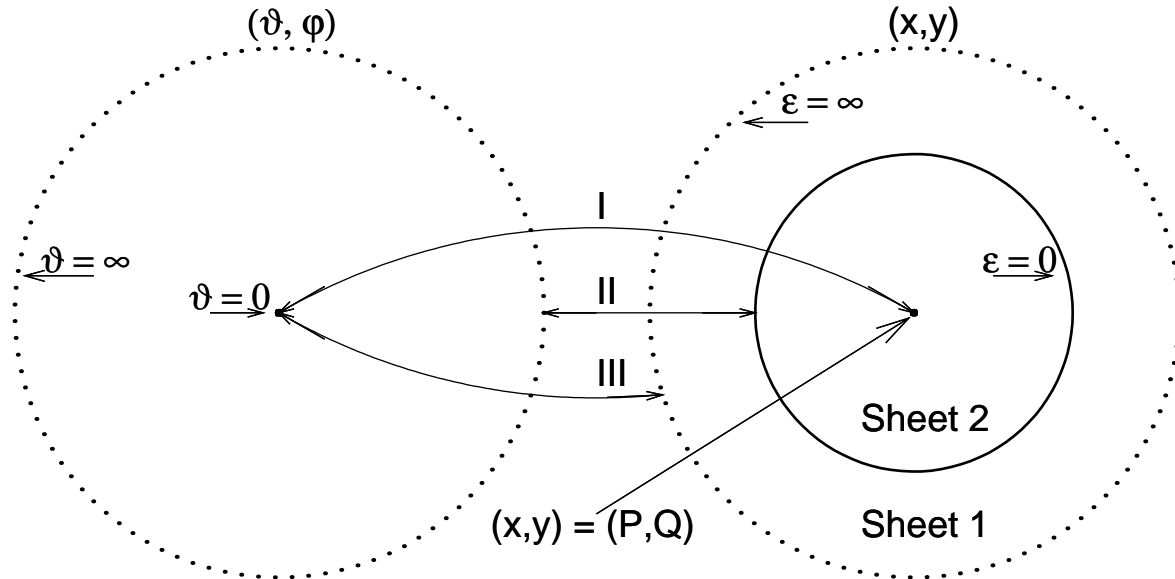


FIG. 1: Relations between the  $(\vartheta, \varphi)$ - and  $(x, y)$  maps of a constant- $(t, z)$  surface in (2.8) and (5.1). The arrow marked by I corresponds to the transformation (5.4) that maps the set  $\vartheta = 0$  to  $(x, y) = (P, Q)$ . Arrow II shows that both (5.3) and (5.4) map  $\vartheta \rightarrow \infty$  to the circle  $\mathcal{E} = 0$ . Arrow III corresponds to (5.3) that maps  $\vartheta = 0$  to  $\mathcal{E} \rightarrow \infty$ .

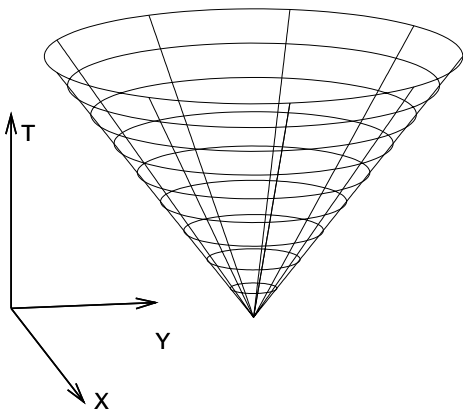


FIG. 2: The surface of constant  $z = z_1$  and constant  $\varphi = \varphi_0$  in a spacetime with the metric (5.1). The embedding is in a Minkowskian 3-space with the metric (6.4). The vertex at  $R = 0$  lies at the Big Bang. The circles represent the surfaces of constant  $t$  and  $z$  in (5.1). This embedding is not a one-to-one representation, the surface in the figure is covered with that of (6.3) an infinite number of times – see explanation in the text.

Now we go back to (6.2) and consider a surface of constant  $\vartheta = \vartheta_0$ . Writing  $C_0 = \sinh \vartheta_0$  we can write the 2-metric as

$$ds_{z_1, \vartheta_0}^2 = \left[ C_0^2 + \left( \frac{dt}{dR} \right)^2 \right] dR^2 - d(C_0 R)^2 - (C_0 R)^2 d\varphi^2, \quad (6.10)$$

and then the embedding equations are

$$T = \int \sqrt{C_0^2 + \left( \frac{dt}{dR} \right)^2} dR$$

$$\begin{aligned} &\equiv C_0 \int \sqrt{1 + \frac{R}{2EC_0^2 R + 2MC_0^2}} dR, \\ X &= C_0 R \cos \varphi, \quad Y = C_0 R \sin \varphi. \end{aligned} \quad (6.11)$$

Now there is no multiple covering because  $\varphi$  is a cyclic coordinate also in spacetime, and the surface given by (6.11) looks qualitatively similar to that in Fig. 2, except that the presence of  $C_0$  introduces some flexibility. The second line of (6.11) shows that the explicit expression for  $T$  is (6.7) multiplied by  $C_0$ , with  $(M, E)$  replaced by  $C_0^2(M, E)$ . The radius of a circle of constant  $R$  is now  $(C_0 R)$ . The value of  $C_0$  is any in  $(-\infty, +\infty)$ . When  $C_0 \rightarrow 0$ , the surface degenerates to the straight line  $X = Y = 0$ . In order that  $C_0 T$  in (6.7) allows a well-defined limit  $C_0 \rightarrow 0$ , the constant  $D$  must have the form

$$D = \frac{M \ln C_0}{C_0 E \sqrt{2E(2EC_0^2 + 1)}} + \frac{D_1}{C_0}, \quad (6.12)$$

where  $D_1$  is another constant. Again, it may be chosen so that  $C_0 T = 0$  at  $R = 0$ .

From (6.11) we find

$$\lim_{C_0 \rightarrow \infty} \frac{dT}{d(C_0 R)} = 1, \quad (6.13)$$

so in the limit  $C_0 \rightarrow \infty$  the surface (6.11) becomes exactly a cone with the vertex angle  $\pi/4$ . However, with  $C_0 \rightarrow \infty$  the whole cone recedes to infinity, as can be seen from (6.7) and (6.11): the vertex of the cone, which is at  $R = 0$ , has the property  $\lim_{C_0 \rightarrow \infty} (C_0 T)|_{R=0} = \infty$ , even with the value of  $D$  corrected as in (6.12).

Note that the image in Fig. 2 will not change qualitatively when we go over from the hyperbolically symmet-

ric subcase (5.1) to the general (nonsymmetric) quasi-hyperbolic case (2.7) – (2.8). Each hypersurface of constant  $z$  in it is axially symmetric, and its metric can be transformed to the form (6.2). Moreover, any surface of constant  $z$  and  $y$  can have its metric transformed to the form (6.3). The only change with respect to Fig. 2 is that the cone-like surfaces, while still being axially symmetric, can have their vertex angles different at different values of  $z$ .

For completeness, we now consider the special flat hypersurface with  $R_{,t} = 1$ ,  $M = 0$  and  $E = 1/2$  mentioned below (6.1). It can be all transformed to the 3-dimensional Minkowski form. The transformation to the Minkowski coordinates  $(\tau, X, Y)$  is

$$\begin{aligned} \tau &= R \cosh \vartheta, & X &= R \sinh \vartheta \cos \varphi, \\ Y &= R \sinh \vartheta \sin \varphi. \end{aligned} \quad (6.14)$$

The surfaces of constant  $R$  are given by the equation

$$\tau^2 - X^2 - Y^2 = R^2. \quad (6.15)$$

These are two-sheeted hyperboloids when  $R > 0$  and a cone when  $R = 0$ . They intersect the  $\tau$ -axis horizontally, and all tend asymptotically to the cone  $R = 0$  as  $X^2 + Y^2 \rightarrow \infty$  (see Fig. 3).

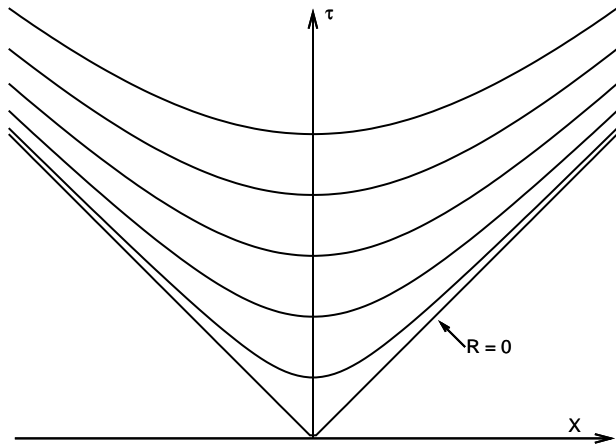


FIG. 3: An axial cross-section through the family of hyperboloids given by (6.15).

The surface  $\varphi = 0$  of (6.14) is depicted in Fig. 4. Note, however, that Figs. 3 and 4 are graphs of a Lorentzian space mapped into an Euclidean space, so geometrical relations of (6.2) are not faithfully represented.

### B. The $R(t, z)$ curves

Where  $M > 0$ , we have  $R_{,tt} < 0$  from (2.9) with  $\Lambda = 0$ . Consequently,  $R$  as a function of  $t$  must be concave. The slopes of the curves  $R(t, z)$  at various  $z$  depend on  $E(z)$ ,

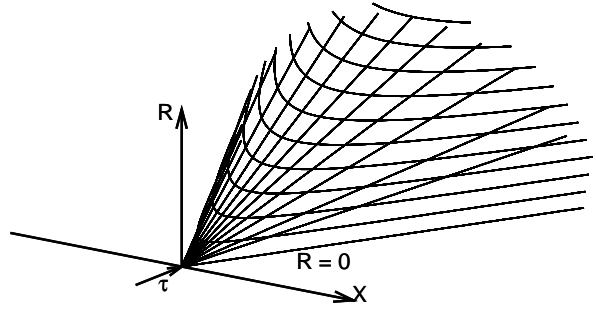


FIG. 4: The subspace  $\{z = \text{constant}, \varphi = 0\}$  of the spacetime (5.1) with  $R = t$ . The hyperbolae are curves of different constant values of  $R$ , the straight lines emanating from the origin are lines of constant  $\vartheta$ .

and their initial points at  $t = t_B$  are determined by  $t_B(z)$ , so both can vary arbitrarily when we proceed from one value of  $z$  to another. Fig. 5 shows a 3-d graph of an example of a family of  $R(t, z)$  curves corresponding to different values of  $z$ .

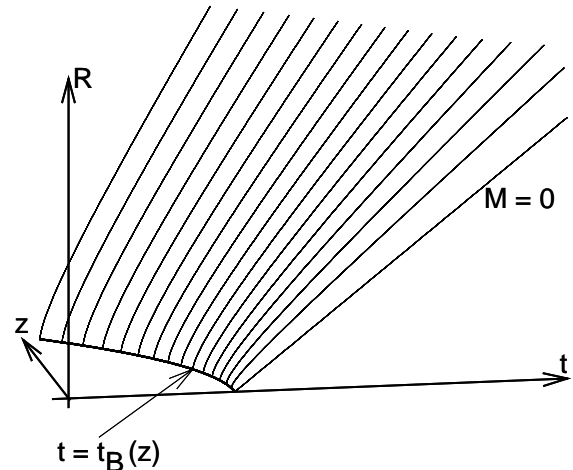


FIG. 5: An exemplary collection of the  $R(t, z)$  curves for various fixed values of  $z$ . The bang time curve  $t = t_B(z)$  must be a decreasing function of  $z$  to avoid shell crossings [1]. The rightmost line is straight, corresponding to  $M = 0$ . The other  $t(R)$  functions in this figure are given by (3.5) with  $t_B(z) = 2 - 0.05z^2$ . They have  $M$  increasing with  $z$  (so  $|R_{,tt}|$  is increasing as a function of  $z$ ) and  $E$  increasing with  $z$  (so  $R_{,t}$  is increasing). The values of  $(M, E)$  increase from  $(0.0, 0.6)$  in increments of  $(0.1, 0.1)$ . Note that all curves except the  $M = 0$  one hit the  $t = t_B$  set with  $R_{,t} \rightarrow \infty$ .

### C. Hypersurfaces of constant $t$

Formulae for the curvature of the spaces of constant  $t$  in (2.7) – (2.8) are (from Ref. [1], in notation adapted to that used here):

$${}^3R_{1212} = {}^3R_{1313}$$

$$= -\frac{R(R_{,z} - R\mathcal{E}_{,z}/\mathcal{E})(E_{,z} - 2E\mathcal{E}_{,z}/\mathcal{E})}{(2E - 1)\mathcal{E}^2},$$

$${}^3R_{2323} = -\frac{2ER^2}{\mathcal{E}^4}, \quad (6.16)$$

where the coordinates are labelled as  $(x^1, x^2, x^3) = (z, x, y)$ . Equations (6.16) show that a space of constant  $t$  becomes flat when  $E = 0$ , but then it has the Lorentzian signature  $(+ - -)$ . Consequently, with the Euclidean signature, these spaces can never be flat.

Now let us consider the surfaces  $H_2$  of constant  $t = t_0$  and  $\varphi = \varphi_0$  in (5.1). For the beginning we will assume that  $R_{,z} > 0$  for all values of  $z$  in the region under investigation. Then we can write the metric of  $H_2$  as follows:

$$ds_2^2 = \frac{[dR(t_0, z)]^2}{2E - 1} + R^2 d\vartheta^2. \quad (6.17)$$

When  $E \equiv 1$ , this is the metric of the Euclidean plane in polar coordinates  $(R, \vartheta)$ . With some other constant values of  $E$ , this will be the metric of a cone (see below). With other functional forms of  $E$ , it is the metric of a rotationally symmetric curved surface on which  $\vartheta$  is the polar angular coordinate. We encounter here the same phenomenon that was described in connection with Fig. 2: in each case, a point of coordinates  $(R, \vartheta)$  and points of coordinates  $(R, \vartheta + 2\pi n)$ , where  $n$  is any integer, are projected onto the same point of the plane, cone or curved surface, respectively. However, as before, these points do not coincide in the spacetime (5.1). Examples of embeddings of  $H_2$  in the Euclidean  $E^3$  are illustrated in Fig. 6.

Note that with  $E = \text{constant} \neq 1$  other interesting geometries come up. If we interpret  $\vartheta$  as a polar coordinate, then the ratio of a circumference of a circle  $R = \text{constant}$  to its radius is  $2\pi\sqrt{2E - 1}$ , which means that the surfaces (6.17) are ordinary cones when  $1/2 < E < 1$ , and cone-like surfaces that cannot be embedded in a Euclidean space when  $E > 1$ . With  $E$  being a function of  $z$ , the cones and/or cone-like surfaces are tangent to the  $(z, \vartheta)$  surfaces at the appropriate values of  $z$ . Thus, with  $E > 1$ , the  $(z, \vartheta)$  surfaces cannot be embedded in a Euclidean space. Whether this surface looks like the smooth surface of revolution in the lower panel of Fig. 6, or like a cone, depends on the behaviour of  $E(z)$  in the neighbourhood of the axis  $R = 0$ . But attention: if the value of  $t_0$  under consideration is such that  $t_0 > t_B(z)$  for all  $z$ , then the set  $R = 0$  is not contained in the space  $t = t_0$ . We will come back to this below. We can discuss the embedding when we write the metric (6.17) as

$$ds_2^2 = \frac{2(1 - E)}{2E - 1} dR^2 + dR^2 + R^2 d\vartheta^2. \quad (6.18)$$

Now it is seen that with  $1/2 < E < 1$  we can embed this surface in the Euclidean space with the metric  $ds_3^2 = dX^2 + dY^2 + dZ^2$  by

$$X = R \cos \vartheta, \quad Y = R \sin \vartheta, \quad Z = \pm \int \sqrt{\frac{2(1 - E)}{2E - 1}} dR, \quad (6.19)$$

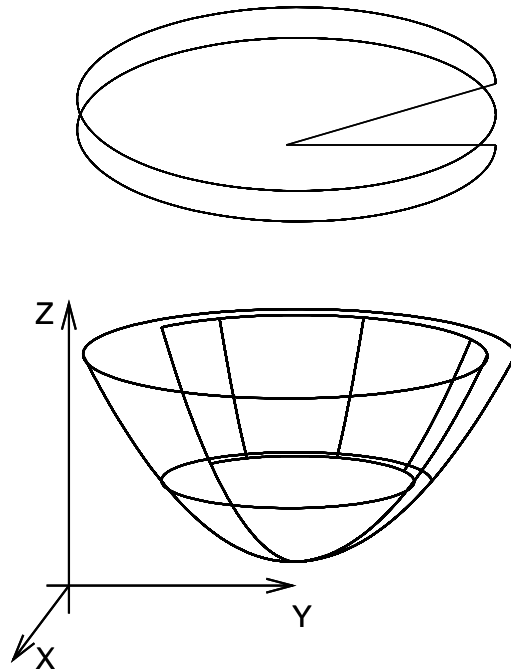


FIG. 6: **Upper graph:** A surface  $H_2$  of constant  $t$  and  $\varphi$  in the metric (5.1) in the case when  $E \equiv 1$ . It is locally isometric to the Euclidean plane, but points having the coordinates  $(R, \vartheta + 2\pi n)$  do not coincide with the point of coordinates  $(R, \vartheta)$ , so the projection of  $H_2$  covers the Euclidean plane multiply. The multiple covering is depicted schematically. **Lower graph:** When  $E$  is not constant, the embedding of a surface of constant  $t$  and  $\varphi$  in the Euclidean space is locally isometric to a curved surface of revolution, with a similar multiple covering, also shown schematically. The surface in the figure is the paraboloid  $Z = R^2$  that results when  $E(z(R)) = (2R^2 + 1)/(4R^2 + 1)$ , where  $z(R)$  is the inverse function to  $R(t_0, z)$ .

while with  $E > 1$  we can embed it in the Minkowskian space with the metric  $ds_3^2 = -dT^2 + dX^2 + dY^2$  by

$$X = R \cos \vartheta, \quad Y = R \sin \vartheta, \quad T = \pm \int \sqrt{\frac{2(E - 1)}{2E - 1}} dR, \quad (6.20)$$

For later reference let us note, from (6.19), that  $dZ/dR \rightarrow 0$  when  $E \rightarrow 1$  and  $|dZ/dR| \rightarrow \infty$  when  $E \rightarrow 1/2$ . This observation will be useful in drawing graphs and interpreting them.

The surfaces on which  $t$  and  $\vartheta$  are constant look similar to the surfaces described above, with two differences:

1. The coordinate  $\varphi$  changes from 0 to  $2\pi$  also in the spacetime (5.1), so there is no multiple covering of the surfaces in the Euclidean space.

2. The circumference to radius ratio is this time  $2\pi \sinh \vartheta \sqrt{2E - 1}$ , so the transition from cones to cone-like surfaces occurs at  $\sinh \vartheta = 1/\sqrt{2E - 1}$ .

Now let us recall what was said in the paragraph containing (3.4):  $R(t, z)$  becomes zero *only* at  $t = t_B$ . At any  $t > t_B$ ,  $R > 0$  for all  $z$ , even at  $M = 0$  as (3.6) shows. Thus, the surfaces in Fig. 6 can extend down to the axis  $R = 0$  only if, at the given instant  $t = t_1$ , the function  $t_B(z)$  attains the value  $t_1$  at some  $z = z_1$ : then



$t = t_B$  at  $z = z_1$ , so  $R(t_1, z_1) = 0$ . This is illustrated in Fig. 7. If  $t_2 > t_B(z)$  at all  $z$ , then  $R(t_2, z)$  is nowhere zero. Let  $R_0 > 0$  be the smallest lower bound of  $R(t_2, z)$ ; then  $R(t_2, z) \geq R_0 > 0$  at all  $z$ , and the surface shown in Fig. 6 has a hole of radius  $R_0$  around the axis. Since  $R_{,t} > 0$ ,  $R_0$  is an increasing function of  $t$ , and the radius of the hole increases with  $t$ . This is illustrated in Fig. 8.

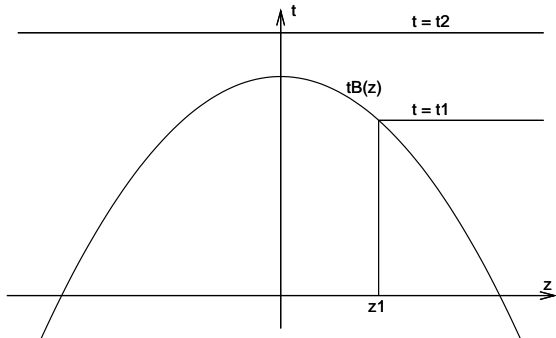


FIG. 7: The hypersurface  $t = t_1$  has a nonempty intersection with the Big Bang set  $t = t_B(z)$ . The function  $R(t_1, z)$  attains the value 0 at  $z = z_1$ , and the surface from Fig. 6 extends down to the axis  $R = 0$ . At  $t = t_2$  we have  $t > t_B$  at all values of  $z$ , so  $R(t_2, z)$  is nowhere zero and has a smallest lower bound  $R_0 > 0$ . This means that the corresponding surface from Fig. 6 will have a hole of radius  $R_0$  around the axis. Since  $R_{,t} > 0$ , the radius of the hole increases with time, as shown in Fig. 8.

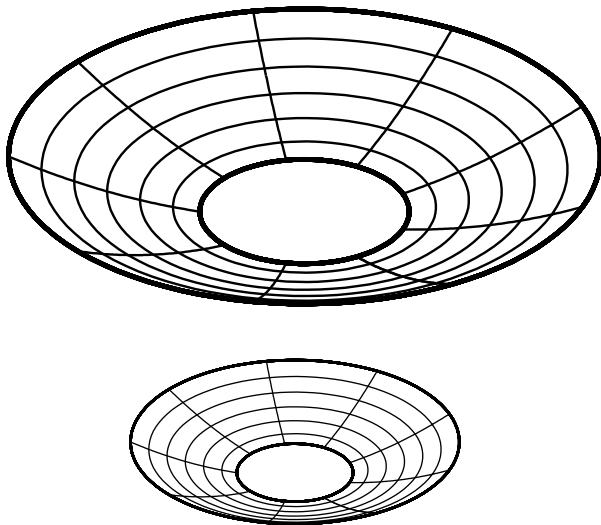


FIG. 8: The surface of constant  $t$  and  $\varphi$  of (5.1), from the bottom graph in Fig. 6, depicted at two instants  $t_2 > t_B$  (bottom graph) and  $t_3 > t_2$  (top graph). The multiple covering of the paraboloid is no longer taken into account. The hole around the axis expands along with the whole surface.

So far, we have considered  $R$  as an independent variable within the space  $t = t_0$ . Since it is a function of  $z$ ,

the parameter along the radial direction in Figs. 6 and 8 is in fact the coordinate  $z$ . Now let us recall that  $R$  is also a function of  $t$  and that at every  $z$  there exists such a  $t$  ( $t = t_B$ ), at which  $R = 0$ . Thus, as we consider the spaces  $t = t_0$  at consecutive values of  $t_0$ , the surfaces depicted in those figures get gradually “unglued” from the Big Bang set (which is represented by the axis of symmetry  $R = 0$ ), and expand sideways. At the moment, at which  $t_0$  begins to obey  $t_0 > t_B$  for all  $z$ , the surface becomes completely detached from the axis and continues to expand sideways. This is when the hole mentioned above first appears.

Let us also note the double sign in the definition of  $Z$ , (6.19), which was not taken into account in Figs. 6 and 8. It means that each of those surfaces has its mirror-image attached at the bottom. In summary, the evolution of those surfaces progresses as shown in Fig. 9. The functions used for this picture are  $M = 10|z|^3$ ,  $E = 0.6 + 0.5e^{-|z|}$ ,  $t_B = -10^3|z| + 100$ . The time instants are  $(t_1, \dots, t_6) = (1, 50, 100, 300, 500, 700)$ .

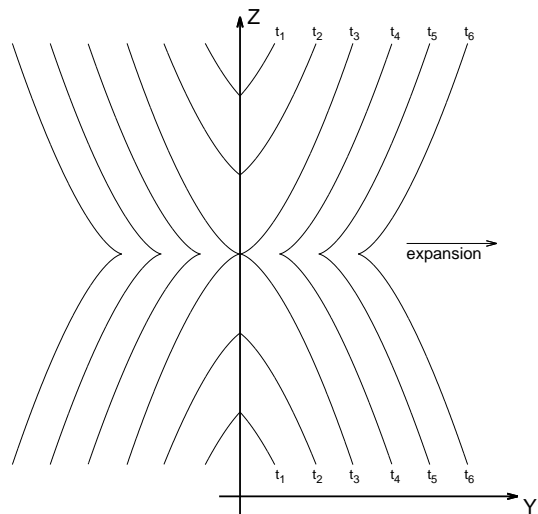


FIG. 9: Evolution of the surface from the lower panel of Fig. 6. The figure shows the axial cross-section of the surface at several time instants,  $t_1 < \dots < t_6$ . The Big Bang goes off along the  $Z$  axis, beginning at the top and at the bottom, and progressing toward the middle. The instant  $t_3$  corresponds to the last moment when the surface has no hole. Multiple covering not shown.

The nondifferentiable cusp at the plane of symmetry is a consequence of the assumption  $R_{,z} > 0$ : to avoid a singularity in the metric (5.1),  $E > 1/2$  must hold everywhere, and then (6.19) implies  $|dZ/dR| < \infty$  everywhere. This means that the upper half of the surface cannot go over smoothly into the lower half.

Let us now consider the case when  $R_{,z} = 0$  at some  $z = z_n$ . To prevent a shell crossing at  $z_n$ ,  $E(z_n) = 1/2$  must also hold, so that  $\lim_{z \rightarrow z_n} (R_{,z} / \sqrt{2E - 1})$  is finite. This implies that  $R_{,z}|_{z_n} = 0$  for all  $t$  (i.e. that the extremum of  $R$  is comoving), and then  $M_{,z} = E_{,z} = 0$  at  $z = z_n$  from (2.9). This is an analogue of a neck – an entity well known from studies of the Lemaître – Tolman model [17].

But, as remarked under (6.20), we have  $dZ/dR \rightarrow \pm\infty$  where  $E \rightarrow 1/2$ . The evolution then looks like in Fig. 10. The functions used for drawing it are  $M = 10^2|z|^3$ ,  $E = 0.5 + |z|^{3/2}$ ,  $t_B = -10^3|z|^2 + 100$ , and the time instants are  $(t_1, \dots, t_6) = (1, 50, 100, 200, 300, 400)$ .

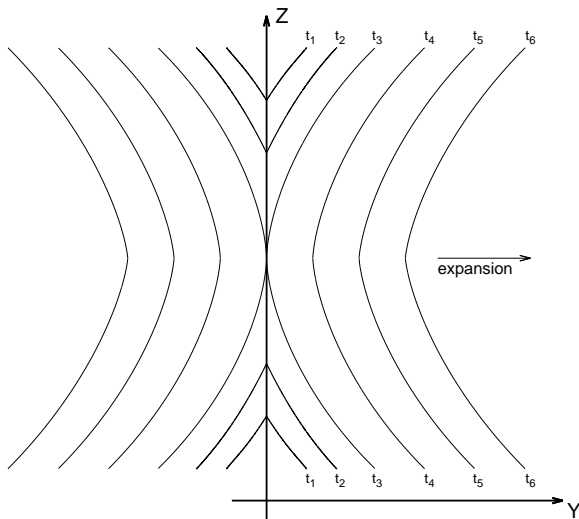


FIG. 10: The analogue of Fig. 9 for the situation when  $R_{,z} = 0$  at some  $z = z_n$  (in the middle horizontal plane). Then the upper half of each constant- $(t, \varphi)$  surface goes over smoothly into the lower half.

The minimum of  $R$  with respect to  $z$  need not exist in any space of constant  $t$ . (By minimum we mean not only a differentiable minimum similar to the one in Fig. 10, but also a cusp at the minimal value like the one in Fig. 9.) It will not exist when the function  $t_B(z)$  has no upper bound, i.e. when the Big Bang keeps going off for ever, moving to ever new locations. In that case, the surfaces shown in the upper half of Fig. 9 will never get detached from the Big Bang set, only the vertex of each conical surface will keep proceeding along the axis. In the special case  $t_B = \text{constant}$ , the whole surface of constant  $t$  and  $\varphi$  gets “unglued” from the axis  $R = 0$  at the same instant. The image would look similar to Fig. 10, but there would be no conical surfaces with the vertices progressing along  $R = 0$ . The generators of the surface in the picture are in general not vertical. They become vertical when  $R_{,z} = 0$  everywhere, i.e. when  $R = R(t)$ , which can happen only in the  $\beta_{,z} = 0$  family of Szekeres solutions that we do not discuss here.

### VII. SPACES OF CONSTANT $t$ IN THE GENERAL QUASI-HYPERBOLIC CASE

The main difference between the hyperbolically symmetric case, where  $\mathcal{E}_{,z} = 0$ , and the full quasi-hyperbolic case, where  $\mathcal{E}_{,z} \neq 0$ , is seen in (2.8). Consider two surfaces  $S_1$  and  $S_2$  such that  $t = t_0 = \text{constant}$  on both,  $z = z_1$  on  $S_1$  and  $z = z_2$  on  $S_2$ . When  $\mathcal{E}_{,z} = 0$ , the

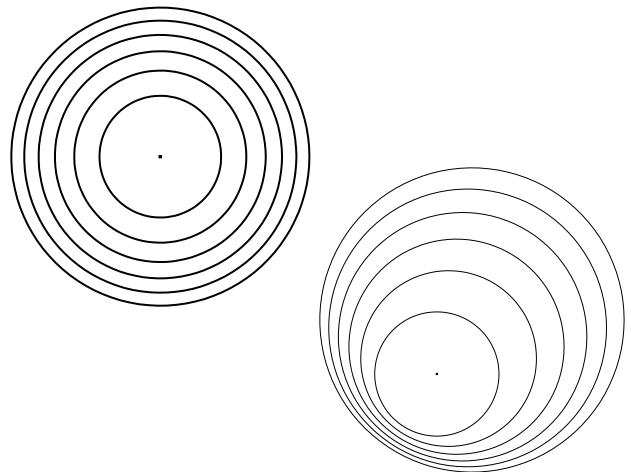


FIG. 11: **Left:** The view from above of the surface from the lower panel in Fig. 6. The circles are images of the curves of constant  $R$  (and thus of constant  $z$ ). **Right:** An example of a corresponding image in the general quasi-hyperbolic case. Now the geodesic distance between the circles depends on the position along the circle.

geodesic distance between  $S_1$  and  $S_2$  along a curve of constant  $(x, y)$  is the same for any  $(x, y)$ . When  $\mathcal{E}_{,z} \neq 0$ , this distance depends on  $(x, y)$  and varies as the functions  $P(z)$ ,  $Q(z)$  and  $S(z)$  dictate. Figure 11, left panel, shows an exemplary family of constant- $R$  curves in a single surface of constant  $t$  and  $\varphi$  with  $\mathcal{E}_{,z} = 0$ . This is a surface of constant  $t$  and  $(y/x)$  in the coordinates of (2.8) – a contour map of the surface from the lower panel in Fig. 6. With a general  $\mathcal{E}(x, y, z)$  the geodesic distance between the constant- $R$  curves will depend on the position along each curve, and the whole family would look like in the lower panel of Fig. 11.<sup>5</sup>

### VIII. INTERPRETATION OF THE MASS FUNCTIONS $M(z)$ AND $\mathcal{M}(z)$ IN THE QUASI-SPHERICAL CASE

In the quasi-spherical case, the function  $M(z)$  of (2.9), by analogy with the Newtonian and the Lemaître – Tolman cases, is understood as the active gravitational mass inside the sphere of coordinate radius  $z$ . In fact, it is puzzling why it depends only on  $z$  when the mass-density (2.10) so prominently depends also on  $t$ ,  $x$  and  $y$ . Somewhat miraculously, as shown below, the denominator in (2.10) is canceled by the  $\sqrt{-g_{11}}$  term inside the integral  $\int \rho \sqrt{|g_3|} d_3x$  that determines the mass in a sphere.<sup>6</sup>

<sup>5</sup> Fig. 11 is in fact deceiving. The curves shown there as circles are images of infinite curves, as explained under (6.5), and each image is covered an infinite number of times.

<sup>6</sup>  $g_3$  is the determinant of the metric of the 3-space  $t = \text{constant}$  in (2.1).

The term containing  $\mathcal{E}_{,z}$  in the numerator gives a zero contribution to the integral. This is consistent with the fact, known from electrodynamics, that the total charge of a dipole is zero (see Refs. [11, 17, 20] for the splitting of (2.10) into the monopole and the dipole part in the quasi-spherical case). It is also consistent with the result of Bonnor [8, 9] that the Szekeres solution can be matched to the Schwarzschild solution.

The considerations of this and the next three sections are intended to prepare the ground for an analogous investigation in the quasi-hyperbolic case further on. The questions we seek to answer are: Can  $M$  still be interpreted as mass, and where does the mass  $M(z)$  reside when a surface of constant  $z$  has infinite surface area?

Let us calculate, in the quasi-spherical case, the amount of rest mass within the sphere of coordinate radius  $z$  at coordinate time  $t$ , assuming that  $z = z_0$  is the center, where the sphere has zero geometrical radius (see Ref. [16]). This amount equals  $\mathcal{M} = \int_{\mathcal{V}} \rho \sqrt{|g_3|} d_3x$ , where  $\mathcal{V}$  is the volume of the sphere and  $\rho$  is the mass density given by (2.10). Substituting for  $\rho$  and  $g_3$  we get

$$\mathcal{M} = \frac{1}{4\pi} \int_{-\infty}^{+\infty} dx \int_{-\infty}^{+\infty} dy \int_{z_0}^z du \left[ \frac{M_{,u}(u)}{\sqrt{1+2E\mathcal{E}^2}} - \frac{3M\mathcal{E}_{,u}}{\sqrt{1+2E\mathcal{E}^3}} \right], \quad (8.1)$$

where  $u$  is the running value of  $z$  under the integral. Note that  $\mathcal{E}$  is the only quantity that depends on  $x$  and  $y$ , it is an explicitly given function, and so the integration over  $x$  and  $y$  can be carried out:

$$\int_{-\infty}^{+\infty} dx \int_{-\infty}^{+\infty} dy \frac{1}{\mathcal{E}^2} = 4\pi, \quad \int_{-\infty}^{+\infty} dx \int_{-\infty}^{+\infty} dy \frac{\mathcal{E}_{,z}}{\mathcal{E}^3} = 0. \quad (8.2)$$

(The first of these just confirms that this is the surface area of a unit sphere.) Using this in (8.1) we get

$$\mathcal{M} = \int_{z_0}^z \frac{M_{,u}}{\sqrt{1+2E}}(u) du, \quad (8.3)$$

which is the same relation as in the LT model,<sup>7</sup> and shows that  $1/\sqrt{1+2E}$  is the relativistic energy defect/excess function (when  $2E < 0$  and  $2E > 0$  respectively).

In the quasi-spherical case we are able to calculate the integral with respect to  $x$  and  $y$  over the whole  $(x, y)$  surface because its surface area is finite. Such a calculation cannot be repeated for the  $\varepsilon \leq 0$  cases because both integrals analogous to (8.2) are infinite. Let us then consider what happens with  $M$  and  $\mathcal{M}$  when we calculate the integrals in (8.2) over a part of the sphere.

## IX. THE MASS IN THE SPHERICALLY SYMMETRIC CASE

In nearly all the papers concerning the LT model and the quasi-spherical Szekeres model it was assumed that each space of constant  $t$  has its center of symmetry (in the LT case) or *origin* (in the quasi-spherical Szekeres case), where  $M = 0$  and  $R = 0$  at all times. We will assume the same here, but *this is an assumption*. It is possible that the center of symmetry is not within the spacetime in the LT case, and the corresponding quasi-spherical Szekeres generalization will then have no “origin”.<sup>8</sup>

For the beginning we will consider the spherically symmetric (Lemaître–Tolman) subcase, in which  $P_{,z} = Q_{,z} = S_{,z} = 0$ , so  $P = Q = 0$  can be achieved by coordinate transformations. Then  $\mathcal{E}_{,z} \equiv 0$  in (8.2). Now suppose that we calculate the integral in the first of (8.2) over a circular patch  $C$  of the sphere (circular in order that no  $(x, y)$  dependence appears from the boundary shape). The boundary of  $C$  is an intersection of the sphere with a cone whose vertex is at the center of the sphere. Let the vertex angle  $\theta$  of the cone be  $\pi/n$ . This translates to the radius of  $C$  in the original  $(x, y)$ -coordinates being  $u_0 = S \tan(\pi/2n) \stackrel{\text{def}}{=} S\beta$ . Then we have in place of the first of (8.2)

$$\begin{aligned} \int_C d_2xy \frac{1}{\mathcal{E}^2} &= 4\pi \frac{u_0^2}{S^2 + u_0^2} \equiv 2\pi [1 - \cos(\pi/n)] \\ &\equiv 4\pi \frac{\beta^2}{1 + \beta^2}. \end{aligned} \quad (9.1)$$

This tends to  $4\pi$  when  $n \rightarrow 1$  ( $u_0 \rightarrow \infty$ ). Note that the final result does not depend on  $S$  – this happened because we have chosen the coordinate radius in each circle,  $\sqrt{x^2 + y^2} = u_0$ , to be a fixed multiple of  $S$ .

In the spherically symmetric case now considered, we choose the same cone to define the circles of integration in (9.1) in all surfaces of constant  $z$ . Instead of (8.3) we get for the amount of rest mass within the cone,  $\mathcal{M}_C$ :

$$\begin{aligned} \mathcal{M}_C &= \frac{1}{4\pi} \int_C d_2xy \int_{z_0}^z du \frac{M_{,u}}{\sqrt{1+2E\mathcal{E}^2}} \\ &= \frac{\beta^2}{1 + \beta^2} \int_{z_0}^z \frac{M_{,u}}{\sqrt{1+2E}}(u) du. \end{aligned} \quad (9.2)$$

The term of (8.1) that contained  $\mathcal{E}_{,u}$  disappeared here in consequence of the assumed spherical symmetry, but it will not disappear when we go over to the general case, and its contribution will have to be interpreted.

<sup>7</sup> For the quasi-spherical case also other integral relations are similar to the ones in the L–T model, which is a consequence of the fact that the dipole contribution vanishes after averaging over x-y surface [27].

<sup>8</sup> The authors are aware of just one paper, in which LT models without a center of symmetry were considered. These are the “in one ear and out the other” and the “string of beads” models of Hellaby [28], described also in Ref. [17]. In both of them,  $M \neq 0$  throughout the space.

## X. SYMMETRY TRANSFORMATIONS OF A SPHERE IN THE COORDINATES OF (2.12)

In the spherically symmetric case rotations around a point are symmetries of the space. In this case, if we rotate the whole cone around its vertex to any other position, eq. (9.2) will not change. Each  $z = \text{const}$  circle will then be rotated by the same angles to its new position, and the result of such a rotation will be a cone isometric to the original one.

However, in the general, nonsymmetric case the spheres  $z = \text{constant}$  are not concentric. Suppose we build, in the general case, a surface composed of circles, each circle taken from a different sphere. If we rotate each sphere by the same angles, whatever surface existed initially, will be deformed into a shape non-isometric to the original one. We want to calculate the effect of such a transformation, and for this purpose we need the formulae for the  $O(3)$  rotations in the  $(x, y)$ -coordinates. We calculate them now.

The generators of spherical symmetry, in the ordinary spherical coordinates, are [17]:

$$\begin{aligned} J_1 &= \frac{\partial}{\partial \varphi}, & J_2 &= \sin \varphi \frac{\partial}{\partial \vartheta} + \cos \varphi \cot \vartheta \frac{\partial}{\partial \varphi}, \\ J_3 &= \cos \varphi \frac{\partial}{\partial \vartheta} - \sin \varphi \cot \vartheta \frac{\partial}{\partial \varphi} \end{aligned} \quad (10.1)$$

We transform these to the  $(x, y)$ -coordinates of (2.12), for the beginning with  $P = Q = 0, S = 1$ , by

$$x = \cot(\vartheta/2) \cos(\varphi), \quad y = \cot(\vartheta/2) \sin(\varphi) \quad (10.2)$$

and obtain

$$\begin{aligned} J_1 &= x \frac{\partial}{\partial y} - y \frac{\partial}{\partial x}, \\ J_2 &= 2xy \frac{\partial}{\partial x} + (1 - x^2 + y^2) \frac{\partial}{\partial y}, \\ J_3 &= (1 + x^2 - y^2) \frac{\partial}{\partial x} + 2xy \frac{\partial}{\partial y}. \end{aligned} \quad (10.3)$$

The transformations generated by  $J_1$  are rotations in the  $(x, y)$ -plane. To find the transformations generated by  $J_3$  we have to solve (see Ref. [17] for explanations):

$$\frac{dx'}{d\lambda} = 1 + x'^2 - y'^2, \quad \frac{dy'}{d\lambda} = 2x'y', \quad (10.4)$$

where  $\lambda$  is the parameter of the group generated by  $J_3$ . The general solution of this is

$$\begin{aligned} y' &= 1/U_1, & U_1 &\stackrel{\text{def}}{=} C + \sqrt{C^2 - 1} \cos(2\lambda + D), \\ x' &= \left[ \sqrt{C^2 - 1} \sin(2\lambda + D) \right] / U_1, \end{aligned} \quad (10.5)$$

where  $C$  and  $D$  are arbitrary constants of integration. These have to obey the initial conditions  $(x', y')|_{\lambda=0} = (x, y)$ . After solving for  $C$  and  $D$  this leads to

$$x' = [2x \cos(2\lambda) + (1 - x^2 - y^2) \sin(2\lambda)] / U_3$$

$$\begin{aligned} U_3 &\stackrel{\text{def}}{=} 1 + x^2 + y^2 + (1 - x^2 - y^2) \cos(2\lambda) \\ &\quad - 2xy \sin(2\lambda), \\ y' &= 2y/U_3. \end{aligned} \quad (10.6)$$

It is instructive to calculate the effect of the transformation (10.6) in the  $(\vartheta, \varphi)$  coordinates of (10.2). Let us then take a point of coordinates  $(x, y) = (x, 0)$ , i.e.  $(\vartheta, \varphi) = (\vartheta, 0)$ , and let us apply (10.6) to it. After a little trigonometry we get

$$\begin{aligned} \tan(\vartheta'/2) &= \frac{1 - \cos \vartheta \cos(2\lambda) - \sin \vartheta \sin(2\lambda)}{\sin \vartheta \cos(2\lambda) - \cos \vartheta \sin(2\lambda)} \\ &\equiv \tan(\vartheta/2 - \lambda) \implies \vartheta' = \vartheta - 2\lambda, \end{aligned} \quad (10.7)$$

i.e. (10.6) is equivalent to rotating the sphere around the  $(\vartheta, \varphi) = (\pi/2, \pi/2)$  axis by the angle  $(-2\lambda)$ .

It can now be verified that the quantity:

$$I(x, y) \stackrel{\text{def}}{=} \frac{1 + x^2 + y^2}{2y} \equiv \frac{1 + x'^2 + y'^2}{2y'} \quad (10.8)$$

is an invariant of the transformation (10.6). The set  $I = 2C$  is the circle  $x^2 + (y - C)^2 = C^2 - 1$ .

An arbitrary circle of radius  $A$  and center at  $x = y = 0$ ,  $x^2 + y^2 = A^2$ , is transformed by (10.6) into the circle

$$\begin{aligned} &\left[ x' - \frac{(1 + A^2) \sin(2\lambda)}{(1 + A^2) \cos(2\lambda) + 1 - A^2} \right]^2 + y'^2 \\ &= \frac{4A^2}{[(1 + A^2) \cos(2\lambda) + 1 - A^2]^2}. \end{aligned} \quad (10.9)$$

The coordinate radius of the  $(x', y')$  circle is different from the original radius  $A$  except when  $\lambda = 0$ , which is the identity transformation. But the coordinate radius is not an invariantly defined quantity. An invariant measure of the circle, its surface area, does not change under the transformation (10.6), and neither does the invariant distance between any two points, as we show below.

The Jacobian of the transformation (10.6) is

$$\frac{\partial(x', y')}{\partial(x, y)} = \frac{4}{U_3^2}. \quad (10.10)$$

Together with (10.8) and (10.6) this shows that the surface element under the integral (9.2),  $4dx dy / \mathcal{E}^2$ , does not change in form after the transformation. (This must be so, since (10.6) is just a change of variables that does not change the value of the integral.) Thus, (10.6) preserves the area of any circle, as is appropriate for a symmetry.

The invariant distance between the points  $(x, y) = (0, 0)$  and  $(x, y) = (A, 0)$  (i.e. the invariant radius of the original circle referred to in (10.9)) is, from (2.7) – (2.8) with  $\varepsilon = +1, P = Q = 0, S = 1$ :

$$\int_0^A \frac{dx}{1 + x^2} = 2 \arctan A. \quad (10.11)$$

The image under (10.6) of any point  $(x, 0)$  is  $(x_1(x), 0)$ , where, from (10.6):

$$x_1(x) = \frac{2x \cos(2\lambda) + (1 - x^2) \sin(2\lambda)}{1 + x^2 + (1 - x^2) \cos(2\lambda) - 2x \sin(2\lambda)}. \quad (10.12)$$

Thus, the image of  $(0, 0)$  is  $(x_0, 0)$ , where

$$x_0 = \frac{\sin(2\lambda)}{1 + \cos(2\lambda)}. \quad (10.13)$$

The invariant distance between the images of  $(0, 0)$  and of  $(A, 0)$  is then

$$\int_{x_1(0)}^{x_1(A)} \frac{dx_1}{1 + x_1^2} = 2 \arctan(x_1)|_{x_0}^{x_1(A)} \equiv 2 \arctan A, \quad (10.14)$$

by employing the identity  $\arctan \alpha - \arctan \beta = \arctan [(\alpha - \beta)/(1 + \alpha\beta)]$ . This certifies that the invariant distance between the center of a circle and a point on the circle is the same as the invariant distance between their images (but the image of the center is no longer the center of the image-circle, compare (10.9) and (10.13)).

The transformations generated by  $J_2$  result from those for  $J_3$  by interchanging  $x'$  with  $y'$  and  $x$  with  $y$ ; then all the conclusions about invariant properties follow also

for these transformations, and, in consequence, for any composition of (10.6) with them.

## XI. THE MASS IN THE GENERAL QUASI-SPHERICAL CASE

Now let us consider the general case, and integrals analogous to (8.2), where the  $(x, y)$  integration extends only over a circular subset of each sphere, the radius of each circle being a fixed multiple of  $S$ . In the general case, each sphere has a geometrically preferred center at  $(x, y) = (P(z), Q(z))$ , and, for the beginning, we choose the center of the disc of integration  $C$  at that point. As before, the radius of each circle will be a fixed multiple of  $S$ :  $\sqrt{x^2 + y^2} \stackrel{\text{def}}{=} u_0 = S\beta$ . This means, this time the volume of integration will not be a simple cone, but a ‘wiggly cone’ – the circles in the different  $z = \text{const}$  surfaces will have their centers not on a straight line orthogonal to their planes, but on the curve given by the parametric equations  $x = P(z)$ ,  $y = Q(z)$  that is not orthogonal to the planes of the circles. The result (9.1) still holds within each  $z = \text{const}$  surface, but the analogue of the second integral in (8.1), calculated over the interior of the ‘wiggly cone’ here, will no longer be zero. Instead, introducing in each  $z = \text{const}$  surface the polar coordinates  $x = P + u \cos \varphi$ ,  $y = Q + u \sin \varphi$ , we get

$$\begin{aligned} \int_C d_2xy \frac{\mathcal{E}_{,z}}{\mathcal{E}^3} &= \int_0^{2\pi} d\varphi \int_0^{u_0} u du \frac{(S_{,z}/2) (1 - u^2/S^2) - \frac{1}{S} (P_{,z} u \cos \varphi + Q_{,z} u \sin \varphi)}{(S^3/8) (1 + u^2/S^2)^3} \\ &\equiv 8\pi S S_{,z} \int_0^{u_0} \frac{u S_{,z} (S^2 - u^2)}{(S^2 + u^2)^3} du = 4\pi S S_{,z} \frac{u_0^2}{(S^2 + u_0^2)^2} = 4\pi \frac{S_{,z}}{S} \frac{\beta^2}{(1 + \beta^2)^2}. \end{aligned} \quad (11.1)$$

In agreement with (8.2) this goes to zero when  $u_0 \rightarrow \infty$ . Consequently, from (8.1), (9.2) and (11.1), the total mass within the wiggly cone is

$$\mathcal{M} = \frac{\beta^2}{1 + \beta^2} \int_{z_0}^z \frac{M_{,u}}{\sqrt{1 + 2E}}(u) du - 3 \frac{\beta^2}{(1 + \beta^2)^2} \int_{z_0}^z \frac{M S_{,u}}{S \sqrt{1 + 2E}}(u) du. \quad (11.2)$$

It contains a contribution from  $S_{,z}$  that is decreasing with increasing  $\beta$ , i.e. the greater volume we take, the less significant the contribution from  $S_{,z}$  gets. It will vanish when the integrals extend over the whole infinite range of  $x$  and  $y$  (in the limit  $\beta \rightarrow \infty$ ). This can be interpreted so that in a wiggly cone the dipole components of mass distribution do contribute to  $\mathcal{M}$  – but less and less as the volume of the cone increases. Thus, with such choice of the integration volume  $M$  does not have an immediate interpretation – but it becomes proportional to the mass within the cone in the spherically symmetric limit.

As an example, consider the axially symmetric family of spheres whose axial cross-section is shown in Fig. 12. The circles are given by the equation

$$(x - \sqrt{b^2 + u^2})^2 + y^2 = u^2, \quad (11.3)$$

where  $b$  is a constant that determines the center of the limiting circle of zero radius, while  $u$  is the radius of the circles. (The same family of spheres was used in Ref. [1] to construct Szekeres coordinates for a flat space.) Figure 13, left graph, shows the initial wiggly cone constructed for these spheres – the one referred to in (11.1) and (11.2).

We derived the transformation (10.6) in the coordinates in which the constants  $(P, Q, S)$  were set to  $(0, 0, 1)$  by coordinate transformations. With general values of  $(P, Q, S)$ , the result would be

$$\begin{aligned}
\frac{x' - P}{S} &= \left[ 2 \frac{x - P}{S} \cos(2\lambda) + \left( 1 - \frac{(x - P)^2 + (y - Q)^2}{S^2} \right) \sin(2\lambda) \right] / U_4 \\
y' - Q &= 2 \frac{y - Q}{U_4}, \\
U_4 &\stackrel{\text{def}}{=} 1 + \frac{(x - P)^2 + (y - Q)^2}{S^2} + \left[ 1 - \frac{(x - P)^2 + (y - Q)^2}{S^2} \right] \cos(2\lambda) - 2 \frac{x - P}{S} \sin(2\lambda). \quad (11.4)
\end{aligned}$$

Now let  $z = z_1$  correspond to the base of the wiggly cone, where the values of the arbitrary functions are  $P_1 = P(z_1)$ ,  $Q_1 = Q(z_1)$  and  $S_1 = S(z_1)$ . Apply the transformation (11.4) with  $(P, Q, S) = (P_1, Q_1, S_1)$  to each sphere intersecting the wiggly cone. In the base  $z = z_1$  this will be a symmetry, in other spheres this will not be a symmetry. One should in principle calculate the effect of this transformation in other spheres on the integrands in (9.2) and (11.1) to see what happens. But then, (11.4) is merely a change of variables under the integral that does not change the value of the calculated integral. Thus, eq. (11.2) applies independently of where we choose the base of the wiggly cone, and its position that we chose initially (each circle had its center in the geometrically distinguished center of the  $(x, y)$ -surface) is only necessary to fix the relation between circles corresponding to different values of  $z$ .

The result of the transformation (11.4) applied to the wiggly cone of the left graph in Fig. 13 is shown in the same figure in the right graph.

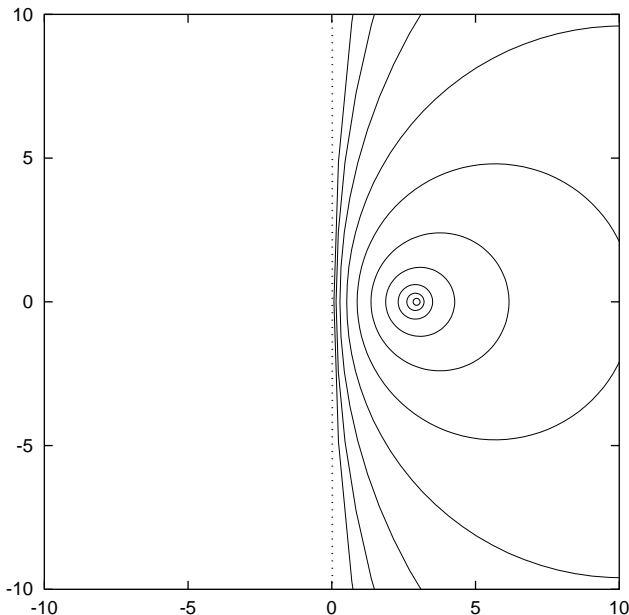


FIG. 12: An axial cross-section through the family of spheres given by (11.3).

## XII. THE SYMMETRY TRANSFORMATIONS IN THE HYPERBOLICALLY SYMMETRIC CASE

Before proceeding to the case of interest, let us consider the hyperbolically symmetric subcase, in which  $P_{,z} = Q_{,z} = S_{,z} = 0$ , and so  $P = Q = 0$  by a transformation of  $x$  and  $y$ . The symmetry group of the resulting metric is a subgroup of that for the corresponding vacuum solution [1]:

$$\begin{aligned}
ds^2 &= - \left( 1 + \frac{2m}{R} \right) dT^2 + \frac{1}{1 + 2m/R} dR^2 \\
&\quad - R^2 (d\vartheta^2 + \sinh^2 \vartheta d\varphi^2), \quad (12.1)
\end{aligned}$$

The full set of Killing vectors for this metric is

$$\begin{aligned}
k_1^\alpha &= \delta_0^\alpha, & k_4^\alpha &= \delta_3^\alpha, \\
k_2^\alpha &= \cos \varphi \delta_2^\alpha - \coth \vartheta \sin \varphi \delta_3^\alpha, \\
k_3^\alpha &= \sin \varphi \delta_2^\alpha + \coth \vartheta \cos \varphi \delta_3^\alpha, \quad (12.2)
\end{aligned}$$

where  $(x^0, x^1, x^2, x^3) = (T, R, \vartheta, \varphi)$ . To find the symmetries explicitly, we have to transform (12.2) to the coordinates of (2.8).

We are interested in the transformations within an  $(x, y)$  surface, and those are generated by  $k_2, k_3$  and  $k_4$ . The transformation from the  $(\vartheta, \varphi)$  coordinates of (12.1) to Sheet 2 of the  $(x, y)$ -coordinates of (2.8) is (5.4). The inverse formulae are

$$\begin{aligned}
\varphi &= \arctan(y/x), \\
\cosh \vartheta &= \frac{1 + x^2 + y^2}{1 - (x^2 + y^2)}, \\
\sinh \vartheta &= \frac{2\sqrt{x^2 + y^2}}{1 - (x^2 + y^2)}. \quad (12.3)
\end{aligned}$$

We now transform the Killing fields (12.2) by (12.3). In the  $(x, y)$ -coordinates we get for the generators

$$J_1 = x \frac{\partial}{\partial y} - y \frac{\partial}{\partial x}, \quad (12.4)$$

$$J_2 = [1 + (y^2 - x^2)] \frac{\partial}{\partial x} - 2xy \frac{\partial}{\partial y}, \quad (12.5)$$

$$J_3 = -2xy \frac{\partial}{\partial x} + (1 + x^2 - y^2) \frac{\partial}{\partial y}. \quad (12.6)$$

The  $J_1$  generates rotations in the  $(x, y)$  surface. To find the transformations generated by  $J_2$ , we have to solve

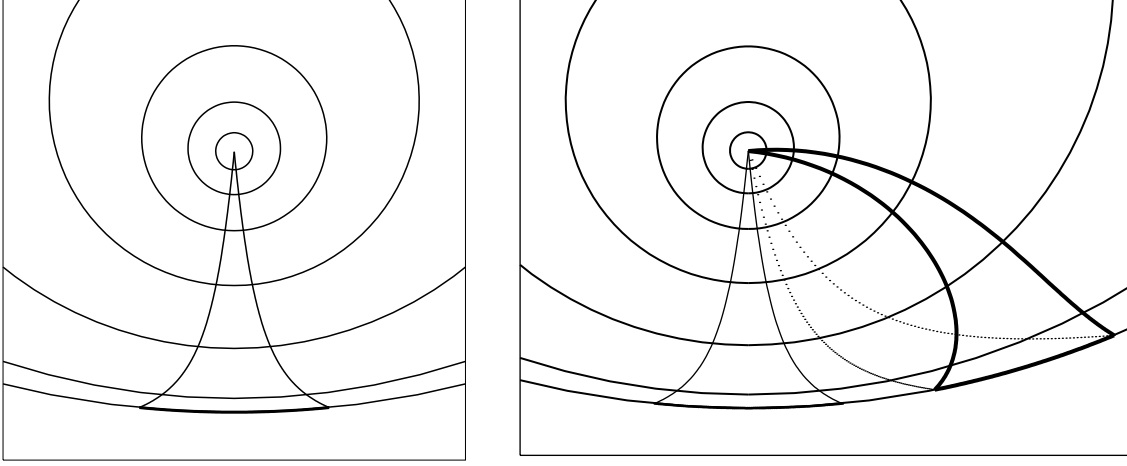


FIG. 13: **Left graph:** a wiggly cone constructed for the family of spheres shown in Fig. 12. The vertex angle for this cone is  $\pi/32$ . **Right graph:** the result of the transformation (11.4) applied to the cone from the left graph. The initial cone is shown in thin lines. The rest mass contained in the new wiggly cone is the same as it was in the initial cone. Dotted lines show the image of the initial cone that would result if each circle of intersection of the original cone with a sphere were rotated by the same angle around the center of its sphere.

the set

$$\frac{dx'}{d\lambda} = 1 + y'^2 - x'^2, \quad \frac{dy'}{d\lambda} = -2x'y', \quad (12.7)$$

with the initial condition that at  $\lambda = 0$  we have  $(x', y') = (x, y)$ . The general solution of this set is

$$\begin{aligned} y' &= 1/W_1, & W_1 &\stackrel{\text{def}}{=} -C + \sqrt{C^2 + 1} \cosh(2\lambda + D), \\ x' &= (1/W_1)\sqrt{C^2 + 1} \sinh(2\lambda + D), \end{aligned} \quad (12.8)$$

where  $C$  and  $D$  are arbitrary constants to be determined from  $x'(0) = x$ ,  $y'(0) = y$ . They are

$$\begin{aligned} \sinh D &= 2x/W_2, & \cosh D &= (x^2 + y^2 + 1)/W_2, \\ W_2 &\stackrel{\text{def}}{=} \sqrt{(x^2 + y^2 - 1)^2 + 4y^2}, \\ C &= \frac{1}{2y} (x^2 + y^2 - 1). \end{aligned} \quad (12.9)$$

So, finally

$$\begin{aligned} x' &= (1/W_3) [2x \cosh(2\lambda) + (1 + x^2 + y^2) \sinh(2\lambda)], \\ W_3 &\stackrel{\text{def}}{=} 1 - (x^2 + y^2) + (1 + x^2 + y^2) \cosh(2\lambda) \\ &\quad + 2x \sinh(2\lambda), \\ y' &= 2y/W_3. \end{aligned} \quad (12.10)$$

The equations corresponding to (12.7) for the generator  $J_3$  result from (12.7) simply by interchanging  $x'$  with  $y'$ . The corresponding initial condition then results by interchanging  $x$  with  $y$ . Thus, from (12.10) we can read off the transformation generated by  $J_3$ ; it is

$$\begin{aligned} x' &= 2x/W_4, \\ W_4 &\stackrel{\text{def}}{=} 1 - (x^2 + y^2) + (1 + x^2 + y^2) \cosh(2\lambda) \end{aligned}$$

$$+ 2y \sinh(2\lambda), \quad (12.11)$$

$$y' = (1/W_4) [2y \cosh(2\lambda) + (1 + x^2 + y^2) \sinh(2\lambda)].$$

Note that the  $(x', y')$  given by (12.10) also obey the third equation in (12.9), so the quantity

$$I_1 \stackrel{\text{def}}{=} \frac{1}{2y} (x^2 + y^2 - 1) \quad (12.12)$$

is an invariant of the transformations (12.10). The corresponding invariant for (12.11) is

$$I_2 \stackrel{\text{def}}{=} \frac{1}{2x} (x^2 + y^2 - 1) \quad (12.13)$$

These facts are helpful in calculations, and so is the following identity that follows from (12.12)

$$x'^2 + y'^2 - 1 \equiv \frac{2}{W_3} (x^2 + y^2 - 1). \quad (12.14)$$

The fact that  $I_1$  is an invariant of (12.10) means that the transformation (12.10) maps the set  $I_1 = C = \text{constant}$  into itself for every  $C$ . This set is a circle of radius  $\sqrt{C^2 + 1}$  and center in the point  $(x, y) = (0, C)$ .

The inverse transformation to (12.10) results from (12.10) by the substitution  $\lambda \rightarrow (-\lambda)$ . This can be verified using the above identities.

These same identities can be used to verify that the transformation (12.10) maps the circle  $x^2 + y^2 = A^2$  into the following circle in the  $(x', y')$ -coordinates

$$\begin{aligned} &\left[ x' - \frac{(1 - A^2) \sinh(2\lambda)}{1 + A^2 + (1 - A^2) \cosh(2\lambda)} \right]^2 + y'^2 \\ &= \frac{4A^2}{[1 + A^2 + (1 - A^2) \cosh(2\lambda)]^2}. \end{aligned} \quad (12.15)$$

The radius of this new circle equals the original radius,  $A$ , only in two cases:  $\lambda = 0$ , which is an identity transformation, or  $A = 1$ . In both cases, also the center of the circle remains unchanged. The radius meant here is a *coordinate radius* that has no invariant meaning. The meaningful quantity is the geometric radius, which is the invariant distance between the center of the circle and a point on its circumference. It can be verified that the invariant distance between any pair of points is the same as the invariant distance between their images.

Below we present some remarks about the transformation (12.10). The same statements apply to (12.11).

The Jacobian of the transformation (12.10) is

$$\frac{\partial(x', y')}{\partial(x, y)} = \frac{4}{W_3^2}, \quad (12.16)$$

which, together with (12.14), shows that the integrand in the integral  $\int d_2xy/\mathcal{E}^2$  is form-invariant under this transformation. In this integral, (12.10) is an ordinary change of variables, and the area of integration in the  $(x', y')$ -variables will be an image of the original area under the same transformation. This means that also the value of this integral is an invariant of (12.10). Thus, if we choose the region of integration to be a circle around a point, it does not matter where the center of the circle is because we can freely move the circle around the  $(x, y)$  surface by symmetry transformations without changing its area.

### XIII. THE MASS FUNCTION IN THE QUASI-HYPERBOLIC CASE

In the quasi-hyperbolic case, the  $(x, y)$  surfaces are infinite, so they do not surround any finite volume. Thus,

unlike in the quasi-spherical case, we should not expect the value of the mass function  $M(z)$  to correspond to a mass contained in a well-defined volume. We should rather observe the analogy to a solid cylinder of finite radius and infinite length in Newton's theory, in which the mass density depends only on the radial coordinate. Its exterior gravitational potential is determined by a function that has the dimension of mass, whose value is proportional to mass contained in a unit of length of the cylinder.

We now proceed by the same plan as we did in the quasi-spherical case. We can freely move a circle of integration around each  $(x, y)$ -surface. We first consider the hyperbolically symmetric case and we erect over a chosen circle a solid column in the  $z$ -direction that contains a certain amount of rest mass. Then we go over to the quasi-hyperbolic nonsymmetric space and erect a wiggly column that contains the same amount of rest mass.

We will integrate over the interior of a circle in Sheet 2 whose radius  $u_0$  is, for the beginning, unknown. We only know that the radius must be smaller than  $S$ , so that the integration region does not intersect the circle where  $\mathcal{E} = 0$  (since, we recall,  $\mathcal{E} = 0$  is the image of infinity, and the integral over a region that includes  $\mathcal{E} = 0$  would be infinite). Thus, instead of (9.1) and (11.1) we have this time

$$\begin{aligned} \int_U d_2xy \frac{1}{\mathcal{E}^2} &= \int_0^{2\pi} d\varphi \int_0^{u_0} \frac{4uS^2}{(u^2 - S^2)^2} du = 4\pi \frac{u_0^2}{S^2 - u_0^2}, \\ \int_U d_2xy \frac{\mathcal{E}_{,z}}{\mathcal{E}^3} &= \int_0^{2\pi} d\varphi \int_0^{u_0} \frac{-8uS^2}{(u^2 - S^2)^3} (u \cos \varphi P_{,z} + u \sin \varphi Q_{,z} + u^2 S_{,z} / (2S) + SS_{,z} / 2) du = \frac{4\pi SS_{,z} u_0^2}{(u_0^2 - S^2)^2}. \end{aligned} \quad (13.1)$$

The first integral in (13.1) will be independent of  $S$  when  $u_0$  is a fixed multiple of  $S$ :

$$u_0 = \beta S, \quad \beta < 1, \quad (13.2)$$

Then

$$\begin{aligned} \int_U d_2xy \frac{1}{\mathcal{E}^2} &= 4\pi \frac{\beta^2}{1 - \beta^2}, \\ \int_U d_2xy \frac{\mathcal{E}_{,z}}{\mathcal{E}^3} &= \frac{4\pi(S_{,z}/S)\beta^2}{(1 - \beta^2)^2}. \end{aligned} \quad (13.3)$$

Instead of (11.2) we now have:

$$\begin{aligned} \mathcal{M} &= \frac{\beta^2}{1 - \beta^2} \int_{z_0}^z du \frac{M_{,u}(u)}{\sqrt{2E - 1}} \\ &\quad - \frac{\beta^2}{(1 - \beta^2)^2} \int_{z_0}^z du \frac{3MS_{,u}}{S\sqrt{2E - 1}}. \end{aligned} \quad (13.4)$$

The meaning of the limits of integration has to be explained here. In the quasi-spherical case, and in the spherically symmetric LT subcase, one usually assumes that each space of constant  $t$  has its center of symmetry,



where  $M = 0 = R$ . As explained at the beginning of Sec. IX, this is an additional assumption – the center of symmetry need not belong to the spacetime. But the center of symmetry, or origin, is the natural reference point at which the mass function has zero value. In the quasi-hyperbolic case now considered, a similar role is played by the set  $M = 0$ , so we will assume that this set exists. Again, as mentioned earlier, this set is a 2-dimensional surface in each space of constant  $t$ , and not a single point.

With this assumption made,  $z_0$  in (13.4) will be the value of  $z$  at which  $M(z_0) = 0$ . In addition, we assume that  $(M_{,u}/\sqrt{2E-1})$  and  $[S_{,u}/(S\sqrt{2E-1})]$  are finite at  $z = z_0$  and in a neighbourhood of  $z_0$ , so that both integrals in (13.4) tend to zero as  $z \rightarrow z_0$ .

These equations are very similar to the corresponding ones in the quasi-spherical case, (11.1) – (11.2), so one is tempted to interpret  $M$ , by analogy with that case, as a quantity proportional to the active gravitational mass contained within a solid (wiggly) tube with circular sections, the radius of a circular section at  $z = z_1$  being  $\beta S(z_1)$ . The base of the tube is in the surface ( $t = t_0 = \text{const}$ ,  $z$ ), its coordinate height is  $(z - z_0)$ , and its top is at  $(t, z) = (t_0, z_0)$ . There is no problem with this interpretation in the hyperbolically symmetric case, where  $S_{,u} = 0$  and the second integral in (13.4) vanishes.

However, there is a significant difficulty when going over to the quasi-hyperbolic case. In the quasi-spherical case we were free to take the limit of the integral extending over the whole sphere, which was  $\beta \rightarrow \infty$ . Here, the integral over the whole hyperboloid would correspond to  $\beta \rightarrow 1$ , and in this limit all the integrals (13.1) – (13.4) become infinite. Worse still, the contribution from the dipole – the second integral in (13.4) – tends to infinity *faster* than the monopole component (the first integral), while in the spherical case increasing the area of integration caused decreasing the influence of the dipole.

We can do another operation on (13.4) that will shed some light on the meaning of  $M$ . The volume of the region containing the rest mass  $\mathcal{M}$  is

$$\mathcal{V} = \int_{z_0}^z du \int_U d_2xy \sqrt{|g_3(t, u, x, y)|}, \quad (13.5)$$

where  $g_3$  is the determinant of the metric of the 3-dimensional subspace  $t = \text{constant}$  of (2.1), thus

$$\mathcal{V} = \int_{z_0}^z du \int_U d_2xy \frac{R^2 (R_{,u} - R\mathcal{E}_{,u}/\mathcal{E})}{\sqrt{2E-1}\mathcal{E}^2}. \quad (13.6)$$

This has the same structure as the integral representing  $\mathcal{M}$ . Since  $R$  and  $E$  do not depend on  $x$  and  $y$ , the integration with respect to  $(x, y)$  can be carried out, and by (13.1) – (13.3) we get

$$\begin{aligned} \mathcal{V} &= \frac{4\pi\beta^2}{1-\beta^2} \int_{z_0}^z \frac{R^2 R_{,u}}{\sqrt{2E-1}} du \\ &\quad - \frac{4\pi\beta^2}{(1-\beta^2)^2} \int_{z_0}^z \frac{R^3 S_{,u}}{S\sqrt{2E-1}} du. \end{aligned} \quad (13.7)$$

For the ratio  $\mathcal{M}/\mathcal{V}$  we now calculate two consecutive limits: first  $\beta \rightarrow 1$ , to cover the whole of each  $z = \text{constant}$  hyperboloid, and then  $z \rightarrow z_\infty$ , where  $z_\infty$  is the value of  $z$  at which  $R \rightarrow \infty$ , to cover the whole  $t = \text{constant}$  space. After taking the first limit, we get

$$\lim_{\beta \rightarrow 1} \frac{\mathcal{M}}{\mathcal{V}} = \left[ \int_{z_0}^z \frac{3MS_{,u}}{S\sqrt{2E-1}} du \right] / \left[ 4\pi \int_{z_0}^z \frac{R^3 S_{,u}}{S\sqrt{2E-1}} du \right]. \quad (13.8)$$

Since in general (apart from special forms of the functions involved) both the numerator and the denominator above become infinite when  $z \rightarrow z_\infty$ , we apply the de l'Hopital rule and obtain

$$\lim_{z \rightarrow z_\infty} \lim_{\beta \rightarrow 1} \frac{\mathcal{M}}{\mathcal{V}} = \lim_{z \rightarrow z_\infty} \frac{3M}{4\pi R^3}. \quad (13.9)$$

The l.h.s. of the above is the global average of rest mass  $\mathcal{M}$  per volume. The r.h.s. looks very much like the same type of global average for the active gravitational mass  $M$ , except that it is taken with respect to a flat 3-space.

A very similar result follows when we take  $z \rightarrow z_0$  instead of  $z \rightarrow z_\infty$  in (13.8). Then both the numerator and denominator tend to zero and we obtain

$$\lim_{z \rightarrow z_0} \lim_{\beta \rightarrow 1} \frac{\mathcal{M}}{\mathcal{V}} = \lim_{z \rightarrow z_0} \frac{3M}{4\pi R^3}. \quad (13.10)$$

On the l.h.s here we have a global average of  $\mathcal{M}/\mathcal{V}$  over the  $(x, y)$  surface taken at the value of  $z$  at which  $M = 0$ .

Equation (13.10) results also when the integrals in (13.4) – (13.8) are taken over the interval  $[z_1, z_2]$ , where  $z_0 < z_1 < z_2 < z_\infty$ , and then the limit  $z_2 \rightarrow z_1$  is taken.

All the calculations in this section were done in Sheet 2 of the  $(x, y)$  map. The corresponding results for Sheet 1 are obtained by taking all integrals with respect to  $u$  over the interval  $[u_0, \infty)$  (with  $u_0 > S$  now) instead of  $[0, u_0]$ , substituting  $1/u_0$  for  $u_0$  in (13.1), and  $1/\beta$  for  $\beta$  (with the new  $\beta$  obeying  $\beta > 1$ ) in (13.3), (13.4) and (13.7). Equations (13.8) – (13.10) do not change.

The meaning of the limits on the r.h. sides of (13.9) and (13.10) requires further investigation. Note that they arise from the dipole contributions to mass and volume.

#### XIV. SUMMARY

The aim of this paper was to clarify the geometrical structure of the quasi-hyperbolic Szekeres models [3, 4] given by (2.7) – (2.9), and of the associated hyperbolically symmetric dust model given by (5.1). The main results achieved are the following:

1. Although there exists no origin, where  $R$  would be zero permanently, a set where  $M = 0$  can exist. At this location,  $R_{,t}$  is constant (section III).
2. The whole spacetime is both future- and past- globally trapped (section IV).

3. The geometrical interpretation of the  $(x, y)$  coordinates in a constant- $(t, z)$  surface was clarified in Sec. V. Contrary to an earlier claim [1], this surface consists of just one sheet, doubly covered by the  $(x, y)$  map.
4. The geometries of the following surfaces for the metric (5.1) were shown in illustrations, all of them in Sec. VI:
  - (a)  $z = \text{constant}$ ,  $\varphi = 0$  for (5.1) in Figs. 2 to 4.
  - (b) The collection of  $R(t, z)$  curves in Fig. 5.
  - (c)  $t = \text{constant}$ ,  $\varphi = 0$  for (5.1) in Figs. 6 and 8.

It turned out that the surfaces listed under (a) are locally isometric to ordinary surfaces of revolution in the Euclidean space (in special cases to a plane and a cone) when  $E \geq 1$ , but cover the latter an infinite number of times. When  $1/2 < E < 1$ , they cannot be embedded in a Euclidean space even locally. The values  $E \leq 1/2$  are prohibited by the spacetime signature.

The time evolution of the surfaces under 3(c) was illustrated in Figs. 9 and 10.

5. For the general metric (2.7) – (2.8), the geometry of the surfaces  $t = \text{constant}$ ,  $\varphi = 0$  was investigated in Sec. VII and shown in Fig. 11. The other surfaces listed above are the same as in the hyperbolically symmetric case (5.1).
6. In Secs. VIII to XI a detailed analysis was carried out of the relation between the mass function  $M(z)$  and the sum of rest masses in a volume  $\mathcal{M}(z)$  in the quasi-spherical Szekeres model. The function  $M(z)$  represents the active gravitational mass within a sphere of coordinate radius  $z$ , while  $\mathcal{M}(z)$  is the sum of rest masses of particles contained in the same volume:

$$\mathcal{M} = \int_{\mathcal{V}} \sqrt{|g_3|} \rho d_3x, \quad (14.1)$$

where  $\mathcal{V}$  is any volume in a space of constant  $t = t_0$ ,  $g_3$  is the determinant of the metric in that space and  $\rho$  is the mass density at  $t = t_0$ . The relation (8.3) follows in the limit when  $\mathcal{V}$  is the volume of the whole space  $t = t_0$ . The calculations in Secs. VIII to XI demonstrated how to calculate (14.1) within various relevant volumes.

7. In Secs. XII and XIII calculations analogous to those from Secs. VIII – XI were carried out for the quasi-hyperbolic Szekeres models. The aim was to interpret the function  $M(z)$  in this case by identifying the volume in which the active gravitational mass is contained. Integrals analogous to (14.1) can be calculated, but the full analogy with the quasi-spherical models follows only in the (hyperbolically) symmetric case. In the general case, terms arising from the dipole component of the

mass distribution cause difficulties that were not fully resolved. It has only been demonstrated that the average value of  $\mathcal{M}/\mathcal{V}$  over the whole space  $t = t_0$  is determined by the average value of  $M/V_0$ , where  $V_0$  is the flat space limit of  $\mathcal{V}$ .

This problem requires further investigation, but it is hoped that the results achieved here will be of use for that purpose.

#### Appendix A: The curvature tensor for the metric (5.1)

The formulae given below are the tetrad components of the curvature tensor for the metric (5.1). The tetrad is the orthonormal one given by

$$\begin{aligned} e^0 &= dt, & e^1 &= \frac{R_{,z}}{\sqrt{2E-1}} dz, \\ e^2 &= R d\vartheta, & e^3 &= R \sinh \vartheta d\varphi, \end{aligned} \quad (A1)$$

with the labeling of coordinates  $(t, r, \vartheta, \varphi) = (x^0, x^1, x^2, x^3)$ . The components given below are scalars, so any scalar polynomial in curvature components will be fully determined by them. Since they do not depend on  $\vartheta$ , they have no singularity caused by any special value of  $\vartheta$ .  $\square$

$$R_{0101} = \frac{2M}{R^3} - \frac{M_{,z}}{R^2 F}, \quad (A2)$$

$$R_{0202} = R_{0303} = \frac{1}{2} R_{2323} = -\frac{M}{R^3}, \quad (A3)$$

$$R_{1212} = R_{1313} = \frac{M}{R^3} - \frac{M_{,z}}{R^2 F}. \quad (A4)$$

The formulae in both appendices were calculated by the algebraic program Ortocartan [29, 30].

#### Appendix B: The curvature tensor for the metric (2.8)

The formulae given below are the tetrad components of the curvature tensor for the metric (2.8) with  $\varepsilon = -1$ . The tetrad is the orthonormal one given by

$$\begin{aligned} e^0 &= dt, & e^1 &= \frac{F}{\sqrt{2E-1}} dz, \\ e^2 &= \frac{R}{\mathcal{E}} dx, & e^3 &= \frac{R}{\mathcal{E}} dy, \end{aligned} \quad (B1)$$

with the labeling of coordinates  $(t, z, x, y) = (x^0, x^1, x^2, x^3)$ , where  $\mathcal{E}$  is given by (2.7) and

$$F \stackrel{\text{def}}{=} R_{,z} - R\mathcal{E}_{,z}/\mathcal{E}. \quad (B2)$$

The components given below are scalars, so any scalar polynomial in curvature components will be fully determined by them.

$$R_{0101} = \frac{2M}{R^3} + \frac{3M\mathcal{E}_{,z}}{R^2\mathcal{E}F} - \frac{M_{,z}}{R^2F}, \quad (\text{B3})$$

$$R_{0202} = R_{0303} = \frac{1}{2} R_{2323} = -\frac{M}{R^3}, \quad (\text{B4})$$

$$R_{1212} = R_{1313} = \frac{M}{R^3} + \frac{3M\mathcal{E}_{,z}}{R^2\mathcal{E}F} - \frac{M_{,z}}{R^2F}. \quad (\text{B5})$$

Note that these reproduce (A2) – (A4) when  $\mathcal{E}_{,z} = 0$ .

We wish to find out whether the sets  $\mathcal{E} = 0$  and  $\mathcal{E} \rightarrow \infty$  are curvature singularities. For this purpose it is useful to introduce the coordinates  $(\vartheta, \varphi)$  by (5.3). Since the quantities (B3) – (B5) are scalars, we only need to substitute (5.3) in them. The two suspected sets become  $\vartheta \rightarrow \infty$  and  $\vartheta = 0$ , respectively. After the transformation we have

$$\mathcal{E} = \frac{S}{2 \sinh^2(\vartheta/2)}, \quad (\text{B6})$$

$$\mathcal{E}_{,z} = \frac{S_{,z}}{2 \sinh^2(\vartheta/2)} [1 - 2 \cosh^2(\vartheta/2)]$$

$$- \coth(\vartheta/2) (P_{,z} \cos \varphi + Q_{,z} \sin \varphi). \quad (\text{B7})$$

The only quantity in (B3) – (B5) that depends on  $\vartheta$  is  $\mathcal{E}_{,z}/(\mathcal{E}F)$ . Using (B6) – (B7) we easily find

$$\lim_{\vartheta \rightarrow \infty} \frac{\mathcal{E}_{,z}}{\mathcal{E}F} = \frac{1}{R}, \quad (\text{B8})$$

$$\lim_{\vartheta \rightarrow 0} \frac{\mathcal{E}_{,z}}{\mathcal{E}F} = \frac{1}{R_{,z} + RS_{,z}/S}. \quad (\text{B9})$$

The loci where these can become infinite do not depend on  $\vartheta$ . Hence,  $\vartheta \rightarrow \infty$  and  $\vartheta = 0$  are not curvature singularities, and neither are  $\mathcal{E} = 0$  or  $\mathcal{E} \rightarrow \infty$ .  $\square$

**Acknowledgements** The research for this paper was inspired by a collaboration with Charles Hellaby, initiated in 2006 at the Department of Mathematics and Applied Mathematics in Cape Town. It was supported by the Polish Ministry of Education and Science grant no N N202 104 838.

- 
- [1] C. Hellaby and A. Krasinski, *Phys. Rev.* **D77**, 023529 (2008).
- [2] A. Krasinski, *Phys. Rev.* **D78**, 064038 (2008); + erratum: *Phys. Rev.* **D85**, 069903(E) (2012). Fully corrected version: arXiv:0805.0529v4.
- [3] P. Szekeres, *Comm. Math. Phys.* **41**, 55-64 (1975).
- [4] P. Szekeres, *Phys. Rev. D* **12**, 2941-8 (1975).
- [5] W. B. Bonnor, N. Tomimura, *Mon. Not. Roy. Astr. Soc.* **175**, 85 (1976).
- [6] S. W. Goode and J. Wainwright, *Mon. Not. Roy. Astr. Soc.* **198**, 83 (1982).
- [7] S. W. Goode and J. Wainwright, *Phys. Rev.* **D26**, 3315 (1982).
- [8] W.B. Bonnor, *Nature* **263**, 301 (1976).
- [9] W.B. Bonnor, *Comm. Math. Phys.* **51**, 191-9 (1976).
- [10] W. B. Bonnor, A. H. Sulaiman and N. Tomimura, *Gen. Rel. Grav.* **8**, 549-559 (1977).
- [11] M.M. de Souza, *Rev. Bras. Fiz.* **15**, 379 (1985).
- [12] W. B. Bonnor, *Class. Q. Grav.* **3**, 495 (1986).
- [13] W. B. Bonnor, D. J. R. Pugh, *South Afr. J. Phys.* **10**, 169 (1987).
- [14] P. Szekeres, in: *Gravitational radiation, collapsed objects and exact solutions*. Edited by C. Edwards. Springer (Lecture Notes vol. 124), New York 1980, p. 477.
- [15] K. Bolejko, *Phys. Rev. D* **73**, 123508 (2006).
- [16] C. Hellaby and A. Krasinski, *Phys. Rev. D* **66**, 084011, (2002).
- [17] J. Plebański and A. Krasinski, *An Introduction to General Relativity and Cosmology*, Cambridge U P (2006).
- [18] A. Krasinski, *Inhomogeneous Cosmological Models*, Cambridge U P (1997), ISBN 0 521 48180 5.
- [19] K. Bolejko, A. Krasinski, C. Hellaby, C. and M.-N. Celerier, *Structures in the Universe by exact methods – formation, evolution, interactions*. Cambridge University Press 2009.
- [20] A. Krasinski and K. Bolejko, *Phys. Rev. D* **85**, 124016 (2012).
- [21] R. Kantowski R. K. and Sachs, *J. Math. Phys.* **7**, 443 (1966).
- [22] C. Hellaby, *J. Math. Phys.* **37**, 2892-905 (1996).
- [23] G. F. R. Ellis, in: *Proceedings of the International School of Physics ‘Enrico Fermi’, Course 47: General Relativity and Cosmology*. Edited by R. K. Sachs. Academic Press, New York and London 1971, pp. 104 – 182; reprinted, with historical comments, in *Gen. Rel. Grav.* **41**, 575 (2009).
- [24] Robertson, H. P. and T. W. Noonan (1968). *Relativity and Cosmology*. W. B. Saunders Company, Philadelphia – London – Toronto, p. 374 – 378.
- [25] A. Krasinski, *J. Math. Phys.* **30**, 433 (1989).
- [26] N. Mustapha and C. Hellaby, *Gen. Rel. Grav.* **33**, 455 (2001).
- [27] K. Bolejko, *Gen. Rel. Grav.* **41**, 1585 (2009).
- [28] C. Hellaby, *Class. Quant. Grav.* **4**, 635 (1987).
- [29] A. Krasinski, *Gen. Rel. Grav.* **33**, 145 (2001).
- [30] A. Krasinski, M. Perkowski, *The system ORTOCARTAN – user’s manual*. Fifth edition, Warsaw 2000.